Silesian university in Opava

Mathematical Institute in Opava

Adam Hlaváč

Constant astigmatism equation and surfaces of constant astigmatism

Abstract of the Ph.D. Thesis

December 2017

Geometry and Global Analysis

SLEZSKÁ UNIVERZITA V OPAVĚ

Matematický ústav v Opavě

Adam Hlaváč

Rovnice konstantního astigmatismu a plochy s konstantním astigmatismem

Autoreferát dizertační práce

Prosinec 2017

Geometrie a globální analýza

Výsledky uvedené v této dizertační práci byly získány v průběhu mého doktorského studia oboru Geometrie a globální analýza na Matematickém ústavu Slezské univerzity v Opavě v letech 2010–2017.

Výzkum byl podporován projekty SGS/1/2011, SGS/1/2013, SGS/2/2013, SGS/17/2016 a projektem GAČR P201/11/0356.

Dizertant:	Mgr. Adam Hlaváč Matematický ústav Slezské univerzity v Opavě
Školitel:	doc. RNDr. Michal Marvan, CSc. Matematický ústav Slezské univerzity v Opavě
Školicí pracoviště:	Matematický ústav Slezské univerzity v Opavě
Oponenti:	prof. RNDr. Josef Mikeš, DrSc. Přírodovědecká fakulta Univerzity Palackého v Olomouci prof. E. V. Ferapontov Loughborough University, England

Autoreferát této dizertační práce byl zveřejněn dne 29. prosince 2017.

Státní doktorská zkouška a obhajoba dizertační práce se budou konat dne 28. února 2018 v 9.30 hod před oborovou komisí doktorského studia Geometrie a globální analýza v zasedací místnosti rektorátu Slezské univerzity v Opavě.

Dizertační práce je dostupná v knihovně Matematického ústavu, Na Rybníčku 626/1, 746 01, Opava.

Předseda Oborové rady:	prof. RNDr. Miroslav Engliš, DrSc. Matematický ústav v Opavě Slezská univerzita v Opavě Na Rybníčku 626/1 746 01 Opava

The author is indebted to doc. RNDr. Michal Marvan, CSc. for his guidance and kind supervision over the years. He would also like to thank RNDr. Petr Blaschke, Ph.D. for fruitful discussions.

Contents

1 Historical background and preliminaries

1.1 Surfaces of constant astigmatism

Surfaces of constant astigmatism, i.e. surfaces characterized by the constancy of the difference $\rho_2 - \rho_1$ between the principal radii of curvature ρ_1, ρ_2, were already known by 19th century geometers. Although nameless at that time, they are studied in works by Bianchi [6, 9], Lipschitz [33], von-Lilienthal [32], Ribaucour [44] and Mannheim [35].

Most important results regarding constant astigmatism surfaces are undoubtedly due to Bianchi. In [6] he showed (see also [44]) that evolutes[1] of constant astigmatism surfaces are pseudospherical, i.e. with constant negative Gaussian curvature. In the same paper, he proved that involutes[2] of pseudospherical surfaces corresponding to parabolic geodesic[3] net are of constant astigmatism, see also [8, §136].

Apparently, Bianchi was the first to obtain surfaces of constant astigmatism explicitly, namely surfaces [6, eq. (30)] corresponding to Dini's pseudospherical helicoids (see, e.g., [45, §1.4.2] or [50, p. 183]). For pictures of the surfaces, see Fig. 1.

A remarkable class of constant astigmatism surfaces was studied by Lipschitz [33], see Sect. 4, and its subclass was later investigated by von Lilienthal [32]. Von Lilienthal surfaces coincide with involutes of Beltrami's pseudosphere, for pictures see Fig. 2 or [5, p. 14].

[1] Two *evolutes* (also called *focal surfaces*) of given surface $\mathbf{r}$ with unit normal $\mathbf{n}$ are $\hat{\mathbf{r}}_1 = \mathbf{r} + \rho_1\mathbf{n}$ and $\hat{\mathbf{r}}_2 = \mathbf{r} + \rho_2\mathbf{n}$, where ρ_1, ρ_2 are principal radii of curvature. In other words, evolutes are formed by loci of the centres of curvature for all points of a given surface

[2] Let $\mathbf{r}(X,Y)$ be a surface parameterised by *geodesics,* i.e. the metric is of the form $\mathrm{d}X^2 + g(X,Y)\,\mathrm{d}Y^2$. A family of *involutes* of surface $\mathbf{r}(X,Y)$ is given by $\tilde{\mathbf{r}} = \mathbf{r} + (a - X)\mathbf{r}_X$, where a is arbitrary real constant.

[3] According to [10], geodesic coordinates (X,Y) on a pseudospherical surface $\mathbf{r}(X,Y)$ with Gaussian curvature $K = -1/R^2$ are called *parabolic* if $\mathbf{I} = \mathrm{d}X^2 + \mathrm{e}^{2X/R}\,\mathrm{d}Y^2$, *elliptic* if $\mathbf{I} = \mathrm{d}X^2 + R^2\sinh^2(X/R)\,\mathrm{d}Y^2$ and *hyperbolic* if $\mathbf{I} = \mathrm{d}X^2 + \cosh^2(X/R)\,\mathrm{d}Y^2$.

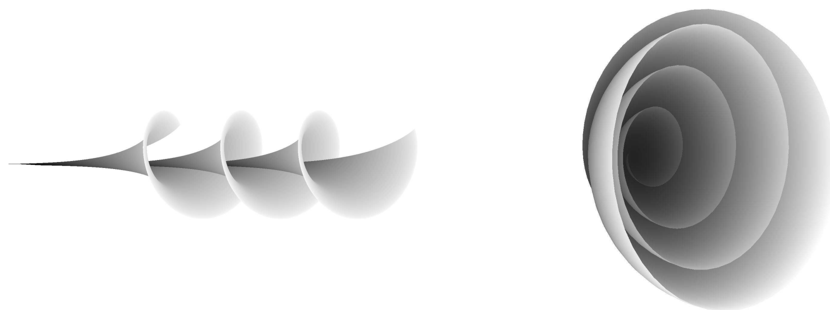

Figure 1: Dini's pseudospherical surface (left) and its constant astigmatism involute (right).

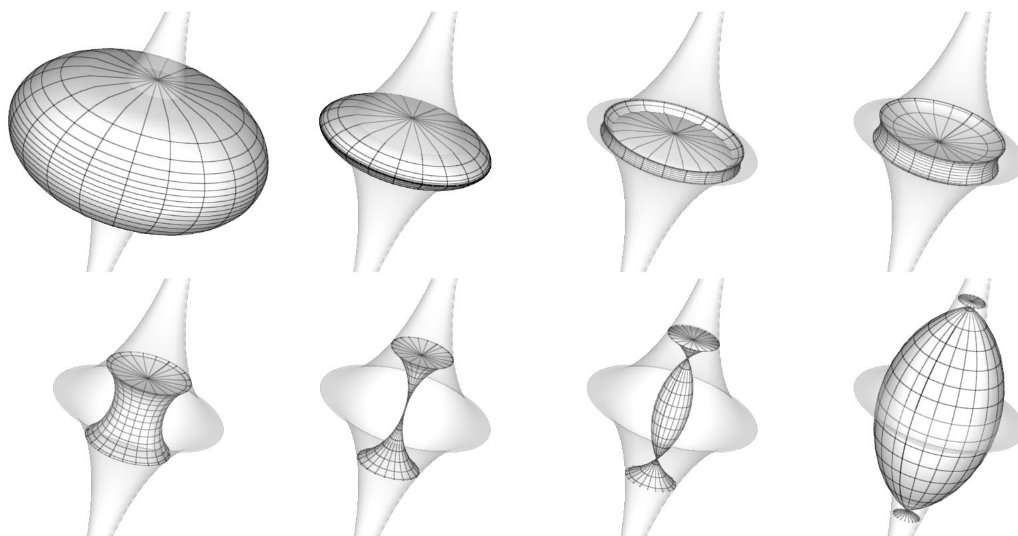

Figure 2: Von Lilienthal surfaces of constant astigmatism and their evolute, the pseudosphere.

To our best knowledge, no result concerning constant astigmatism surfaces appears throughout the twentieth century. One can only speculate why the topic fell into oblivion, however, it reemerged in 2009 in the work [5] concerning the systematic search for integrable classes of Weingarten surfaces.

In the paper, the surfaces were given a name and equation (5) was derived for the first time.

1.2 The constant astigmatism equation

In this section we recall results from [5]. They form necessary background for our approach in this thesis.

We consider surfaces immersed in Euclidean space under parameterisation by the lines of curvature (also known as curvature coordinates). Hence, the fundamental forms can be written as

$$\begin{aligned} &\mathbf{I} = u^2\,\mathrm{d}x^2 + v^2\,\mathrm{d}y^2\,, \quad \mathbf{II} = \frac{u^2}{\rho_1}\,\mathrm{d}x^2 + \frac{v^2}{\rho_2}\,\mathrm{d}y^2\,, \\ &\mathbf{III} = \frac{u^2}{\rho_1^2}\,\mathrm{d}x^2 + \frac{v^2}{\rho_2^2}\,\mathrm{d}y^2\,, \end{aligned} \tag{1}$$

where ρ_1, ρ_2 are the principal radii of curvature. The first two forms determine the surface up to the rigid motions (Bonnet theorem).

Recall that a surface is said to be of *constant astigmatism (CA)* if the difference $\rho_2 - \rho_1$ between the principal radii of curvature is a nonzero constant (if zero, then the surface is a part of the sphere). We assume the ambient space to be scaled so that $\rho_2 - \rho_1 = \pm 1$.

Definition 1.2.1. A parameterisation by lines of curvature is said to be *adapted* if

$$uv\Big(\frac{1}{\rho_1} - \frac{1}{\rho_2}\Big) = \pm 1 \tag{2}$$

holds.

Adapted curvature coordinates are also *geometric* coordinates in the sense of [18] with the arbitrary constant being normalised to ± 1. Every constant astigmatism (more generally, Weingarten) surface can be equipped with an adapted parameterisation by lines of curvature, see [18, Prop. 5.6] or [5]. Henceforth we assume that x, y are adapted coordinates. Then, according to [5], the nonzero coefficients of the three fundamental forms of a surface of constant astigmatism can be expressed through a single variable $z(x, y)$, namely

$$
\begin{aligned}
u &= \frac{z^{\frac{1}{2}}(\ln z - 2)}{2}, \qquad v = \frac{\ln z}{2z^{\frac{1}{2}}}, \\
\rho_1 &= \frac{\ln z - 2}{2}, \qquad \rho_2 = \frac{\ln z}{2}.
\end{aligned} \tag{3}
$$

Obviously, condition (2) is satisfied.

Let $\mathbf{r}(x, y)$ be the surface of constant astigmatism corresponding to $z(x, y)$, let $\mathbf{n}(x, y)$ denote the unit normal vector. Then $\mathbf{r}, \mathbf{n}$ satisfy the Gauss–Weingarten system

$$
\begin{aligned}
\mathbf{r}_{xx} &= \frac{(\ln z) z_x}{2(\ln z - 2)z}\mathbf{r}_x - \frac{(\ln z - 2) z z_y}{2 \ln z}\mathbf{r}_y + \frac{1}{2}(\ln z - 2) z \mathbf{n}, \\
\mathbf{r}_{xy} &= \frac{(\ln z) z_y}{2(\ln z - 2)z}\mathbf{r}_x - \frac{(\ln z - 2) z z_x}{2 \ln z}\mathbf{r}_y, \\
\mathbf{r}_{yy} &= \frac{(\ln z) z_x}{2(\ln z - 2)z^3}\mathbf{r}_x - \frac{(\ln z - 2) z_y}{2z \ln z}\mathbf{r}_y + \frac{\ln z}{2z}\mathbf{n}, \\
\mathbf{n}_x &= -\frac{2}{\ln z - 2}\mathbf{r}_x, \qquad \mathbf{n}_y = -\frac{2}{\ln z}\mathbf{r}_y.
\end{aligned} \tag{4}
$$

Note that $\mathbf{e}_1 = \mathbf{r}_x/u$, $\mathbf{e}_2 = \mathbf{r}_y/v$, and $\mathbf{n} = \mathbf{e}_1 \times \mathbf{e}_2$ constitute an orthonormal frame.

Compatibility conditions of the Gauss–Weingarten system constitute the Gauss–Mainardi–Codazzi system, which in our case reduces to the Gauss equation alone, and coincides with the *constant astigmatism equation (CAE)*

$$
z_{yy} + \left(\frac{1}{z}\right)_{xx} + 2 = 0. \tag{5}
$$

Note that there is a nice geometric interpretation of the variable z, see Sect. 3 below.

For future reference, we single out the solutions

$$
z = c_1^2 - (y + c_2)^2, \qquad z = \frac{1}{c_1^2 - (x - c_2)^2}, \tag{6}
$$

where c_1, c_2 denote arbitrary real constants. They are easy to obtain as the solutions independent of x or y, respectively. Following [5], we call them the *von Lilienthal solutions*, since they correspond to aforementioned surfaces of revolution studied by von Lilienthal [32], see Fig. 2.

1.3 Symmetries of the CAE

For further reference, we also recall a list of symmetries of equation (5). Lie symmetries are completely known, see [5]. They are the x-translation

$$\mathfrak{T}^x_a(x, y, z) = (x + a, y, z),$$

the y-translation

$$\mathfrak{T}^y_b(x, y, z) = (x, y + b, z),$$

and the scaling

$$\mathfrak{S}_c(x, y, z) = (\mathrm{e}^{-c}x, \mathrm{e}^{c}y, \mathrm{e}^{-2c}z),$$

where a, b, c are real parameters. The known discrete symmetries are exhausted by the x-reversal $\mathcal{R}^x(x, y, z) = (-x, y, z)$, the y-reversal $\mathcal{R}^y(x, y, z) = (x, -y, z)$ and the involution (or duality)

$$\mathfrak{I}(x, y, z) = \Big(y, x, \frac{1}{z}\Big). \tag{7}$$

To avoid possible misunderstanding, we stress that $\mathfrak{T}^x, \mathfrak{T}^y, \mathcal{R}^x, \mathcal{R}^y$ should be understood as single symbols, similarly to $\mathfrak{S}, \mathfrak{I}$. Otherwise said, the superscripts refer to the position in the triple (x, y, z).

Translations and reversals correspond to mere reparameterisations of the constant astigmatism surfaces. The scaling symmetry takes a surface to a *parallel surface*, obtained when moving every point of the surface a constant distance along the normal (*offsetting*). The involution swaps the orientation, interchanges x and y, and makes a unit offsetting.

Obviously,

$$\begin{aligned}
&\mathfrak{I} \circ \mathfrak{I} = \mathrm{id}, \\
&\mathfrak{I} \circ \mathfrak{T}^x_a = \mathfrak{T}^y_a \circ \mathfrak{I}, && \mathfrak{I} \circ \mathfrak{T}^y_a = \mathfrak{T}^x_a \circ \mathfrak{I}, \\
&\mathfrak{S}_c \circ \mathfrak{T}^x_a = \mathfrak{T}^x_{a/c} \circ \mathfrak{S}_c, && \mathfrak{S}_c \circ \mathfrak{T}^y_b = \mathfrak{T}^y_{cb} \circ \mathfrak{S}_c, \\
&\mathfrak{S}_c \circ \mathfrak{I} = \mathfrak{I} \circ \mathfrak{S}_{1/c}, \\
&\mathcal{R}^x \circ \mathfrak{S}_{-1} = \mathcal{R}^y.
\end{aligned}$$

Higher order symmetries have been considered in [5] and [41]; they will not be needed in this thesis.

1.4 The sine-Gordon equation

In the similar way as constant astigmatism surfaces are related to the constant astigmatism equation, pseudospherical surfaces are related to famous sine-Gordon equation. Let us consider a pseudospherical surface $\mathbf{r}(\xi, \eta)$, where the parameters ξ, η are both Chebyshev and asymptotic (which is always possible), i.e.,

$$\mathbf{I} = \mathrm{d}\xi^2 + 2\cos\omega\,\mathrm{d}\xi\,\mathrm{d}\eta + \mathrm{d}\eta^2, \quad \mathbf{II} = 2\sin\omega\,\mathrm{d}\xi\,\mathrm{d}\eta.$$

The position vector $\mathbf{r}(\xi, \eta)$ and the unit normal $\mathbf{n}(\xi, \eta)$ satisfy the Gauss–Weingarten system

$$\begin{aligned}
\mathbf{r}_{\xi\xi} &= \omega_\xi(\cot\omega)\mathbf{r}_\xi - \omega_\xi(\csc\omega)\mathbf{r}_\eta, \\
\mathbf{r}_{\xi\eta} &= (\sin\omega)\mathbf{n}, \\
\mathbf{r}_{\eta\eta} &= \omega_\eta(\cot\omega)\mathbf{r}_\eta - \omega_\eta(\csc\omega)\mathbf{r}_\xi, \\
\mathbf{n}_\xi &= (\cot\omega)\mathbf{r}_\xi - (\csc\omega)\mathbf{r}_\eta, \\
\mathbf{n}_\eta &= (\cot\omega)\mathbf{r}_\eta - (\csc\omega)\mathbf{r}_\xi.
\end{aligned} \tag{8}$$

The compatibility conditions of the above system reduce to the sine-Gordon equation

$$\omega_{\xi\eta} = \sin\omega. \tag{9}$$

The aforementioned geometric relationship between constant astigmatism surfaces and pseudospherical surfaces (the latter being evolutes of the former) induces a nonlocal transformation from the CAE to the sine-Gordon equation and vice versa. Explicit formulas can be found in [5], ready to be applied to the sine-Gordon solutions, which are known in abundance; see [2, 17, 40, 42] and references therein. However, the transformations change both the dependent and independent variables, which makes them difficult to apply.

1.5 Bäcklund transformation for the sine-Gordon equation

The *Bäcklund transformation* [4], see also [8, 10], for the sine-Gordon equation (9) takes a solution ω and produces a new solution $\omega^{(\lambda)}$, given by the system

$$
\begin{aligned}
\left(\frac{\omega^{(\lambda)}-\omega}{2}\right)_{\xi} &= \lambda \sin\frac{\omega^{(\lambda)}+\omega}{2}, \\
\left(\frac{\omega^{(\lambda)}+\omega}{2}\right)_{\eta} &= \frac{1}{\lambda} \sin\frac{\omega^{(\lambda)}-\omega}{2},
\end{aligned}
\tag{10}
$$

λ being called a *Bäcklund parameter.* What is more, the superposition formula [7, 10]

$$
\tan\frac{\omega^{(\lambda_1\lambda_2)}-\omega}{4} = \frac{\lambda_1+\lambda_2}{\lambda_1-\lambda_2}\tan\frac{\omega^{(\lambda_1)}-\omega^{(\lambda_2)}}{4}, \tag{11}
$$

see Fig. 3, allows us to obtain the solution $\omega^{(\lambda_1\lambda_2)}$, the Bäcklund transformation of $\omega^{(\lambda_1)}$ with Bäcklund parameter λ_2, by purely algebraic manipulations.

$$
\begin{tikzcd}
 & \omega^{(\lambda_1)} \arrow[dr, "\lambda_2"] & \\
\omega^{(\lambda_1)} \arrow[ur, "\lambda_1"] \arrow[dr, "\lambda_2"'] & & \omega^{(\lambda_1\lambda_2)} \\
 & \omega^{(\lambda_2)} \arrow[ur, "\lambda_1"'] &
\end{tikzcd}
$$

Figure 3: Nonlinear superposition for the sine-Gordon equation.

The Bäcklund transformation of corresponding pseudospherical surface is also well known, see e.g. [45]. Let $\mathbf{r}$ be a pseudospherical surface corresponding to a sine-Gordon solution $\omega(\xi,\eta)$, i.e. $\mathbf{r}(\xi,\eta)$, its unit normal $\mathbf{n}(\xi,\eta)$ and $\omega(\xi,\eta)$ satisfy the Gauss-Weingarten system (8). A Bäcklund transformation $\mathbf{r}^{(\lambda)}$ of the surface $\mathbf{r}$ is

$$
\mathbf{r}^{(\lambda)} = \mathbf{r} + \frac{2\lambda\csc\omega}{1+\lambda^2}\left[\sin\left(\frac{\omega-\omega^{(\lambda)}}{2}\right)\mathbf{r}_{\xi} + \sin\left(\frac{\omega+\omega^{(\lambda)}}{2}\right)\mathbf{r}_{\eta}\right], \tag{12}
$$

where $\omega^{(\lambda)}$ satisfies (10). Substituting $\lambda = 1$ into (12) one obtains a *complementary* pseudospherical surface

$$
\mathbf{r}^{(1)} = \mathbf{r} + \left[\sin\left(\frac{\omega-\omega^{(1)}}{2}\right)\mathbf{r}_{\xi} + \sin\left(\frac{\omega+\omega^{(1)}}{2}\right)\mathbf{r}_{\eta}\right]\csc\omega. \tag{13}
$$

2 Construction of CAE solutions and CA surfaces

2.1 Construction of CAE solution from ω and $\omega^{(\lambda)}$

In [22] we introduced the method of finding a solution of the CAE corresponding to given sine-Gordon solution ω and its Bäcklund transformation $\omega^{(\lambda)}$.

Proposition 2.1.1. *Let $\omega^{(\lambda)}$ be a general solution of system* (10)*. Let*

$$
\begin{aligned}
x_\xi^{(\lambda)} &= \lambda g^{(\lambda)} \sin\frac{\omega^{(\lambda)}+\omega}{2}, & x_\eta^{(\lambda)} &= \frac{1}{\lambda} g^{(\lambda)} \sin\frac{\omega^{(\lambda)}-\omega}{2},\\
y_\xi^{(\lambda)} &= \frac{\lambda}{g^{(\lambda)}} \sin\frac{\omega^{(\lambda)}+\omega}{2}, & y_\eta^{(\lambda)} &= -\frac{1}{\lambda g^{(\lambda)}} \sin\frac{\omega^{(\lambda)}-\omega}{2},\\
g_\xi^{(\lambda)} &= g^{(\lambda)} \lambda \cos\frac{\omega^{(\lambda)}+\omega}{2}, & g_\eta^{(\lambda)} &= g^{(\lambda)} \frac{1}{\lambda} \cos\frac{\omega^{(\lambda)}-\omega}{2}.
\end{aligned}
\tag{14}
$$

Expressing $z^{(\lambda)} = 1/{g^{(\lambda)}}^2$ in terms of $x^{(\lambda)}, y^{(\lambda)}$, one obtains a solution $z(x,y)$ of the CAE.

The solution in question is given in terms of functions $x^{(\lambda)}, y^{(\lambda)}, g^{(\lambda)}$ which will be called *associated potentials* in the sequel.

Moreover, according to [6], considering a dependence of $\omega^{(\lambda)}(\xi,\eta)$ on an integration constant K, potentials $x^{(\lambda)}(\xi,\eta)$ and $g^{(\lambda)}(\xi,\eta)$ can be obtained by algebraic handling and differentiation with respect to K, namely

$$
g^{(\lambda)} = \frac{\mathrm{d}\omega^{(\lambda)}}{\mathrm{d}K}, \qquad x^{(\lambda)} = -2\frac{\mathrm{d}\ln g^{(\lambda)}}{\mathrm{d}K}.
\tag{15}
$$

Nevertheless, computing $y^{(\lambda)}(\xi,\eta)$ requires integration of the second pair of equations in the system (14).

Recall that potentials $x^{(\lambda)}$ and $y^{(\lambda)}$ are the adapted curvature coordinates on corresponding surface of constant astigmatism.

2.2 Construction of CA surface from pseudospherical surfaces $\mathbf{r}$ and $\mathbf{r}^{(1)}$

In [22] we observed that surfaces of constant astigmatism are easier to obtain from a pair of complementary pseudospherical surfaces $\mathbf{r}$ and $\mathbf{r}^{(1)}$ than from a single pseudospherical surface (as considered in [5]).

Proposition 2.2.1. *Let $\omega^{(1)}(\xi,\eta)$ be a general solution of system* (10) *with $\lambda = 1$ and let $\mathbf{r}^{(1)}$ and $\mathbf{r}$ are related by* (13)*. Then*

$$\tilde{\mathbf{n}} = \mathbf{r}^{(1)} - \mathbf{r} \tag{16}$$

is the unit normal of the corresponding constant astigmatism surface. The constant astigmatism surface itself (having surfaces $\mathbf{r}$ and $\mathbf{r}^{(1)}$ as evolutes) is then given by

$$\tilde{\mathbf{r}} = \mathbf{r} - \ln g^{(1)}\tilde{\mathbf{n}}. \tag{17}$$

2.3 Superposition formula for the CAE

It is natural to ask whether the superposition formula (11) has its analog on the level of CAE solutions. The answer is positive as we showed in [22] and further augmented in [25].

Let us slightly change the notation. Let $\omega^{[0]} = \bar{\omega}^{[0]}$ be a solution of the sine-Gordon equation. Fix Bäcklund parameters $\lambda_1, \ldots, \lambda_{k+1}$ and, according to the diagram

$$\begin{tikzcd}
\omega^{[0]} \arrow[r, "\lambda_2"] \arrow[d, "\lambda_1"'] & \bar{\omega}^{[1]} \arrow[r, "\lambda_3"] \arrow[d, "\lambda_1"'] & \bar{\omega}^{[2]} \arrow[r, "\lambda_4"] \arrow[d, "\lambda_1"'] & \bar{\omega}^{[3]} \arrow[r, "\lambda_5"] \arrow[d, "\lambda_1"'] & \bar{\omega}^{[4]} \arrow[r, "\lambda_6"] \arrow[d, "\lambda_1"'] & \cdots \\
\omega^{[1]} \arrow[r, "\lambda_2"] & \omega^{[2]} \arrow[r, "\lambda_3"] & \omega^{[3]} \arrow[r, "\lambda_4"] & \omega^{[4]} \arrow[r, "\lambda_5"] & \omega^{[5]} \arrow[r, "\lambda_6"] & \cdots,
\end{tikzcd} \tag{18}$$

denote

$$\omega^{[k]} = \omega^{(\lambda_1\lambda_2\ldots\lambda_k)}, \qquad \bar{\omega}^{[k]} = \omega^{(\lambda_2\lambda_3\ldots\lambda_{k+1})}. \tag{19}$$

The diagram is nothing but an extension of that from Fig. 3. In this notation, the superposition formula (11) turns out to be

$$\tan\frac{\omega^{[j+2]} - \bar{\omega}^{[j]}}{4} = \frac{\lambda_1 + \lambda_{j+2}}{\lambda_1 - \lambda_{j+2}} \tan\frac{\omega^{[j+1]} - \bar{\omega}^{[j+1]}}{4}.$$

Proposition 2.3.1. *Let $g^{[j]}, x^{[j]}, y^{[j]}$ be associated potentials corresponding to the pair $\bar{\omega}^{[j-1]}, \omega^{[j]}$. They satisfy recurrences*

$$
\begin{aligned}
x^{[j+1]} &= \frac{\lambda_{j+1}\lambda_1}{\lambda_{j+1}^2 - \lambda_1^2}\left(x^{[j]} - \frac{2\lambda_{j+1}\lambda_1 \sin\dfrac{\bar{\omega}^{[j]} - \omega^{[j]}}{2}}{\lambda_{j+1}^2 + \lambda_1^2 - 2\lambda_{j+1}\lambda_1 \cos\dfrac{\bar{\omega}^{[j]} - \omega^{[j]}}{2}} g^{[j]}\right), \\
y^{[j+1]} &= \frac{\lambda_{j+1}^2 - \lambda_1^2}{\lambda_{j+1}\lambda_1} y^{[j]} - \frac{2}{g^{[j]}} \sin\frac{\bar{\omega}^{[j]} - \omega^{[j]}}{2}, \\
g^{[j+1]} &= \frac{-\lambda_{j+1}\lambda_1}{\lambda_{j+1}^2 + \lambda_1^2 - 2\lambda_{j+1}\lambda_1 \cos\dfrac{\bar{\omega}^{[j]} - \omega^{[j]}}{2}} g^{[j]}.
\end{aligned}
\tag{20}
$$

The recurrences are easy to solve, see Sect. 7. Recall that $z^{[k]} = 1/{g^{[k]}}^2$ expressed in terms of $x^{[k]}$ and $y^{[k]}$ is a solution of the CAE for all k.

Remark 2.3.1. To find a $(k+1)$-th solution $(x^{[k+1]}, y^{[k+1]}, z^{[k+1]})$ of the CAE one needs to know a k-th solution $(x^{[k]}, y^{[k]}, z^{[k]})$, a Bäcklund parameter λ_{k+1} and, additionally, corresponding sine-Gordon solutions $\omega^{[k]}$ and $\bar{\omega}^{[k]}$. On the other hand, in the the case when $\lambda_i = \pm 1$ one can employ *reciprocal transformations,* see Sect. 5. They are immediately applicable to solutions of the constant astigmatism equation with no apriori given sine-Gordon counterpart. However, the computation of path-independent line integral is required.

3 Orthogonal equiareal patterns and slip line fields

3.1 Orthogonal equiareal patterns

The geometric meaning of the variable z can be seen from the third fundamental form which (when substituting (3) into (1)) turns out to be simply

$$\mathbf{III} = z\,\mathrm{d}x^2 + \frac{1}{z}\,\mathrm{d}y^2.$$

Since $\mathbf{III} = \mathrm{d}\mathbf{n}\cdot\mathrm{d}\mathbf{n}$ coincides with the first fundamental form of the Gaussian sphere $\mathbf{n}(x, y)$, it follows that one obtains a rather special parameterisation of the latter. Note that the same result was obtained by Bianchi [9, §375, eq. (20)] in the context of pseudospherical congruences.

Definition 3.1.1. By an *orthogonal equiareal pattern* on a surface S we shall mean a parameterisation x, y such that the corresponding first fundamental form is

$$\mathbf{I}_S = z\,\mathrm{d}x^2 + \frac{1}{z}\,\mathrm{d}y^2, \tag{21}$$

z being an arbitrary function of x, y.

The system of local coordinates $(x, y) = (x^1, x^2)$ from the Def. 3.1.1 obviously satisfies $g_{12} = 0$, $\det g = 1$. Hence, the area element is simply $\mathrm{d}x^1 \wedge \mathrm{d}x^2$ and the area of the curvilinear rectangle $a^i \le x^i \le b^i$, $i = 1, 2$, is equal to $(b^1 - a^1)(b^2 - a^2)$. It follows that the curvilinear rectangles formed by "uniformly spaced" coordinate lines are of equal area, which explains the terminology.

Example 3.1.1. *The Archimedean projection.* A simple example of an orthogonal equiareal pattern on the sphere, that can be seen in the left part of Fig. 4, is delivered by the well-known Archimedean projection of the cylinder $(\cos y, \sin y, x)$ onto an inscribed sphere. In this case, (x, y) is sent to $(\sqrt{1 - x^2}\,\cos y, \sqrt{1 - x^2}\,\sin y, x)$ and we have

$$\mathbf{I}_{\mathrm{Arch}} = \frac{\mathrm{d}x^2}{1 - x^2} + (1 - x^2)\,\mathrm{d}y^2,$$

i.e., one reveals von Lilienthal solution $z = 1/(1 - x^2)$, cf. (6).

Not only every constant astigmatism surface generates an orthogonal equiareal parameterisation of the unit sphere; a converse statement is also available.

Proposition 3.1.1. *Let* $\mathbf{n}(x, y)$, $\|\mathbf{n}\| = 1$, *be an orthogonal equiareal pattern on the unit sphere* S. *Then* z *defined by formula* (21) *is a solution of the constant astigmatism equation* (5).

In the case of S being a plane, the notion of an orthogonal equiareal pattern was introduced by Sadowski [47, 48] in the context of two-dimensional plasticity. Choosing the vectors ∂_x, ∂_y along the *principal stress directions* (i.e., eigenvectors of the stress tensor σ^i_j), Sadowski derived the equiareal property from the equilibrium condition $\operatorname{div} \sigma = 0$ and the Tresca yield condition $\sigma^1_1 - \sigma^2_2 = \text{const}$.

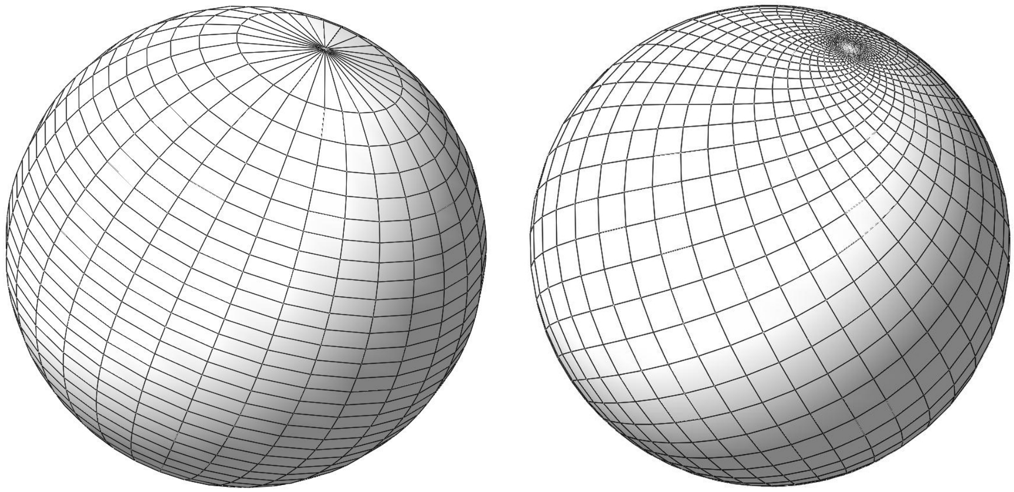

Figure 4: The Archimedean equiareal parameterisation of the unit sphere (left) and corresponding slip line field composed of loxodromes (right).

3.2 Slip line fields

Consider the decomposition of a stress σ on a unit sphere into a sum of the *normal* stress σ_N and the *shear* stress σ_T. The lines along the maximal shear stress direction are called *slip lines* and, as we showed in [22], have a constant deviation of $\frac{1}{4}\pi$ from the principal stress directions.

Definition 3.2.1. By a *slip line field* associated with the orthogonal equiareal pattern (21) on a surface S we shall mean a parameterisation ξ, η such that the angle between ∂_x and ∂_ξ as well as the angle between ∂_y and ∂_η is equal to $\frac{1}{4}\pi$.

Note that slip line field also forms an orthogonal net. What is more, it is not a pure coincidence that the symbols ξ, η from Def. 3.2.1 occur in sine-Gordon equation (9).

Proposition 3.2.1. *Let $\omega^{(1)}(\xi, \eta)$ be a general solution of system* (10) *with $\lambda = 1$ and let $(x, y, z) = (x^{(1)}(\xi, \eta), y^{(1)}(\xi, \eta), 1/g^{(1)}(\xi, \eta))$ is formed by general solutions of system* (14) *with $\lambda = 1$. Let $\tilde{\mathbf{n}}$ be given by* (16)*. Then $\tilde{\mathbf{n}}(x, y)$ is an orthogonal equiareal pattern on the unit sphere while $\tilde{\mathbf{n}}(\xi, \eta)$ is the associated slip line field.*

The meaning of the previous proposition is illustrated in Fig. 5.

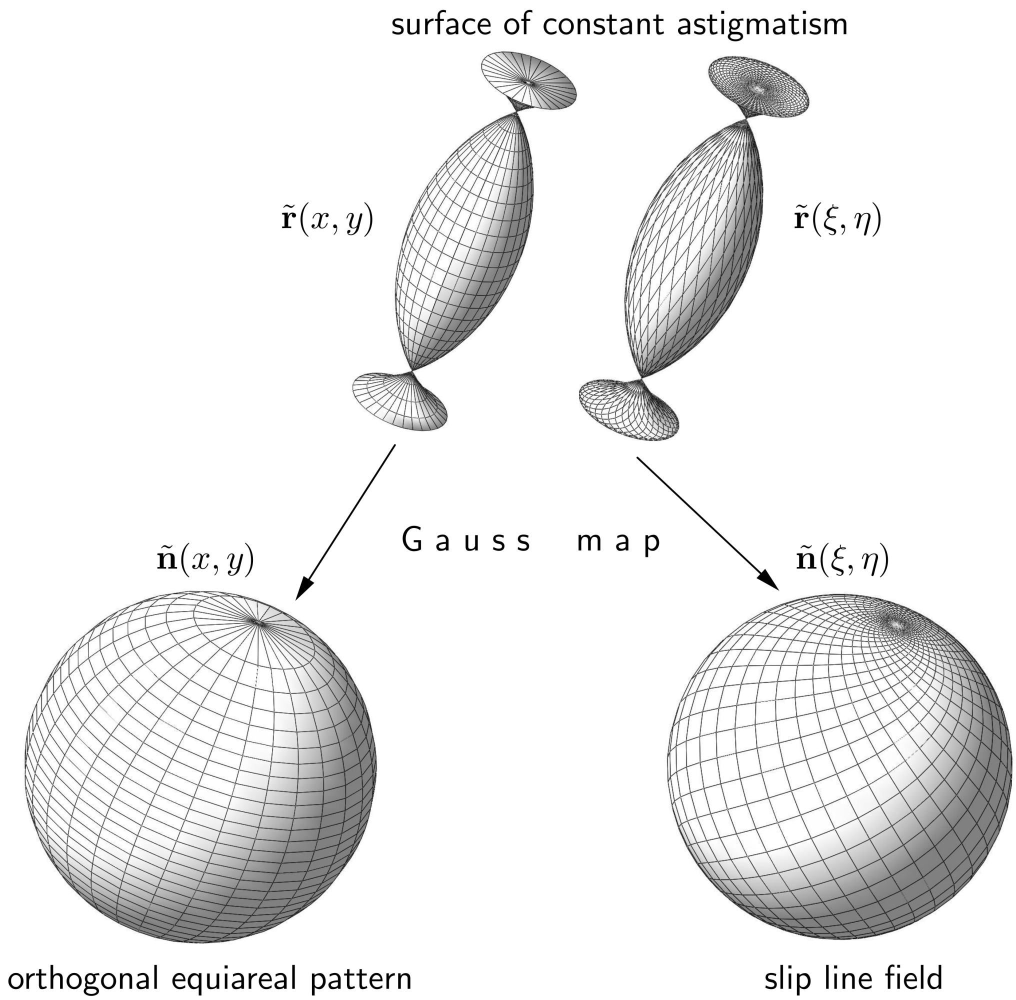

Figure 5: Gaussian map of a constant astigmatism surface.

Example 3.2.1. Continuing Example 3.1.1, we easily see that the corresponding orthogonal net of slip lines is, by definition, formed by the $\pm 45°$ loxodromes (lines of constant bearing); see the right part of Fig. 4 or model No. 249 in the Göttingen collection [46]. Also compare with Zelin's superplastic sheet stretched with a spherical punch [56, Fig. 5b]. Note that corresponding sine-Gordon solution is $\omega^{(1)} = 4 \arctan[\exp(\xi+\eta+c)]$, the Bäcklund transformation of zero solution $\omega = 0$, see Sect. 7.

3.3 Geometrical admissibility of solutions

The next definition is motivated by formula (21). In order to yield metric, z must be real and positive.

Definition 3.3.1. We shall say that a solution z is *geometrically admissible,* if there exists a nonempty open subset $\mathcal{D} \subseteq \mathbb{R}^2$ such that

$$z(x, y) > 0$$

for all $(x, y) \in \mathcal{D}$.

The positivity of z is also necessary and sufficient for the existence of the corresponding constant astigmatism surface. The necessity follows from formula (21) for the Gaussian image, the sufficiency follows from [5, Eq. (26)].

4 Lipschitz solutions of the CAE

In this section we summarize results from the work [23].

4.1 Lipschitz surfaces from 1887

In 1887 Lipschitz in his work [33] presented a class of surfaces of constant astigmatism in terms of spherical coordinates of the Gaussian image $\mathbf{n} = (\cos\phi \sin\theta, \sin\phi \sin\theta, \cos\theta)$. Lipschitz defines a *position angle (Stellungswinkel)* to be the angle σ between $\mathbf{n}_\theta$ and $\mathbf{n}_x$. The Lipschitz class is specified by letting σ depend solely on the latitude θ.[4]

The surfaces are given by [33, Eq. 14] and as a special case they contain von Lilienthal surfaces of revolution, see Fig. 2. A few particular Lipschitz surfaces are plotted in Fig. 6.

[4]Let us quote Lipschitz's original words: "Ich suche jetzt die Oberflächen zu ermitteln, für welche die Differenz $(\rho_2 - \rho_1)$ constant ist, ferner der Stellungswinkel σ nicht von der Variable ϕ und nur von der Variable θ abhängt."

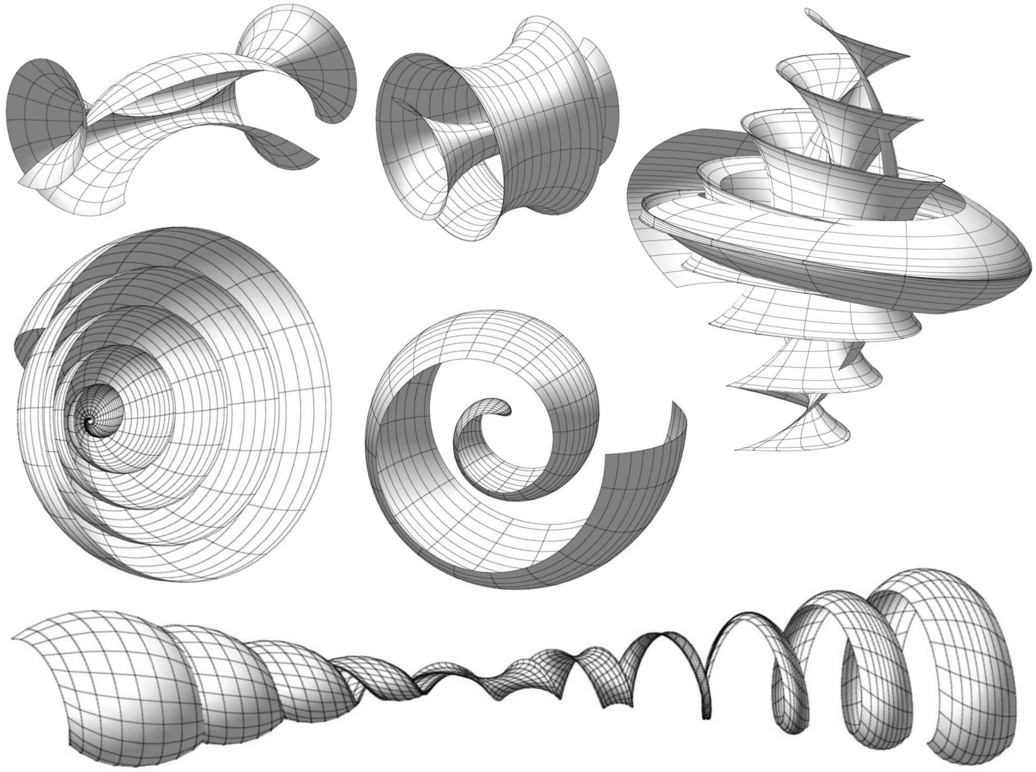

Figure 6: Lipschitz surfaces of constant astigmatism. In the left, one can clearly identify the involute of Dini's surface, cf. Fig. 1.

4.2 Solutions of the CAE corresponding to Lipschitz surfaces

It is not easy to see what are the corresponding solutions $z(x, y)$ and $\omega(\xi, \eta)$. However, since the position angle σ depends solely on θ, we are able to rederive the Lipschitz class in terms of the orthogonal equiareal patterns and compute the corresponding solutions $z(x, y)$ of the CAE. They will be called *Lipschitz solutions*. A generic Lipschitz solution is two-valued and depends on four real parameters.

Theorem 4.2.1. *The general Lipschitz solution of the constant astigmatism equation* (5) *depends on four real parameters* $h_{11}, h_{10}, h_{01}, h_{00}$ *and is a nonzero* *root of the quadratic polynomial*

$$h_y^2 z^2 + (h^2 - 1)z + h_x^2, \tag{22}$$

where

$$h = h_{11}xy + h_{10}x + h_{01}y + h_{00},$$
$$h_y = h_{11}x + h_{01}, \quad h_x = h_{11}y + h_{10},$$

under the condition that h is not a constant (i.e., at least one of the coefficients h_{11}, h_{10}, h_{01} is not zero).

Remark 4.2.1. In terms of $a = h_{11}$ and $b = h_{11}h_{00} - h_{10}h_{01}$, the polynomial (22) becomes

$$h_y^2 z^2 + (h^2 - 1)z + \frac{(ah - b)^2}{h_y^2}$$

and its roots are

$$z = \frac{1 - h^2 \pm \sqrt{(1 - h^2)^2 - 4(ah - b)^2}}{2h_y^2}, \tag{23}$$

whenever $h_y \neq 0$. Formula (23) gives all solutions except the x-dependent von Lilienthal solution (6).

A thorough examination of (23) yields a description of geometrically admissible Lipschitz solutions.

Proposition 4.2.1. *The Lipschitz solution z is geometrically admissible if and only if either $|b| < |a|$ or $|b| < \frac{1}{2}(a^2 + 1)$, $|a| < 1$ (the grey area in Fig.* 7*).*

It also turns out that Lipschitz solutions exactly match the Lie symmetry invariant solutions.

Proposition 4.2.2. *The class of Lipschitz solutions* (22) *coincides with the class of solutions invariant under linear combinations of the Lie symmetries $\mathfrak{T}^x, \mathfrak{T}^y, \mathfrak{S}$.*

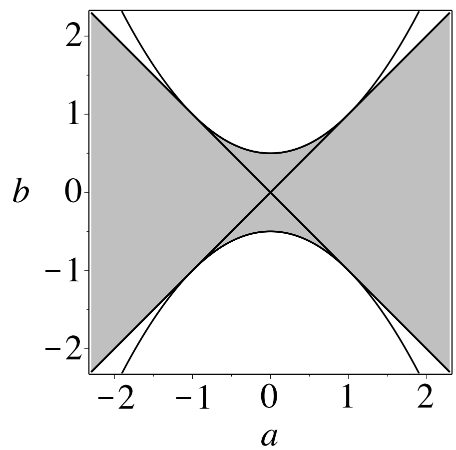

Figure 7: The domain of positivity of z (grey) in a neighbourhood of $a = 0$, $b = 0$.

4.3 Orthogonal equiareal patterns

The orthogonal equiareal patterns corresponding to Lipschitz surfaces are also available.

Proposition 4.3.1. *Denote*

$$E_{a,b} = \int_{h_0}^{h} \frac{\sqrt{(1-\chi^2)^2 - 4(a\chi - b)^2}}{2(a\chi - b)(1-\chi^2)}\,\mathrm{d}\chi, \tag{24}$$

choosing the lower integration limit h_0 so that $E_{a,b}$ is real. Then the orthogonal equiareal pattern corresponding to the general Lipschitz solution is given by the unit vector $\mathbf{n} = (\cos\phi\sin\theta, \sin\phi\sin\theta, \cos\theta)$, where $\theta = \arccos h$ and

$$\begin{aligned} \phi &= \frac{1}{2a}\ln\frac{h_x}{h_y} \pm E_{a,b} \quad \text{if } a \neq 0, \\ \phi &= \frac{h_{01}y - h_{10}x + h_{00}}{2b} \pm E_{0,b} \quad \text{if } a = 0,\ b \neq 0. \end{aligned} \tag{25}$$

A few particular examples are examined in Subsect. 4.5.

4.4 Sine-Gordon solutions and slip lines

In the Subsect. 4.2 we employed the Lipschitz condition: the angle σ between $\mathbf{n}_\theta$ and $\mathbf{n}_x$ on the unit sphere depended solely on θ. Considering the fact that the angle between $\mathbf{n}_x$ and $\mathbf{n}_\xi$ is constant (equal to $\pi/4$), it is clear that in the Lipschitz case the angle σ' between $\mathbf{n}_\theta$ and $\mathbf{n}_\xi$ depends solely on θ as well.

Proposition 4.4.1. *Solutions of the sine-Gordon equation* (9) *corresponding to Lipschitz solutions of the CAE satisfies*

$$\omega_\xi = k\omega_\eta,$$

k being a constant, which means that the solutions are of the form $\omega(k\xi + \eta + \mathrm{const})$.

Thus, ω is nothing but the well-known travelling wave solution (see, e.g., [28, Sect. 3]) also known as a "fluxon chain". The analytic expressions for ω through the Jacobi elliptic functions are recalled in Sect. 8, Remark 8.1.1.

4.5 Examples of Lipschitz solutions

The von Lilienthal case of $a = b = 0$ in (23) corresponds to the global Archimedean parameterisation of the sphere except the poles, see Example 3.1.1.

More examples are easy to construct if the integral (24) can be expressed in terms of elementary functions. This is the case when either $|b| = |a|$, which is admissible if and only if $|a| < 1$, or $|b| = \frac{1}{2}(1 + a^2)$, which is never admissible.

Example 4.5.1. Let $0 < |b| = |a| < 1$, $h_{10} = h_{01} = 0$ and $h_{00} = 1$. Then the solution (23) is of the form

$$z = -\frac{axy(axy + 2) \pm \sqrt{y^2a^2x^2(axy + 2)^2 - 4(b - a - a^2xy)^2}}{2a^2x^2}$$

and the corresponding orthogonal equiareal pattern can be written, using Prop. 4.3.1, as $(\cos\phi\sin\theta, \sin\phi\sin\theta, \cos\theta)$, where $\theta = \arccos(axy+1)$ and

$$\begin{aligned}
\phi = {} & \mp\frac{\sqrt{1-a^2}}{2a}\ln\frac{1-2a^2 \pm h + \sqrt{1-a^2}\sqrt{(h\mp 1)^2 - 4(a^2\mp h)}}{h\mp 1} \\
& - \frac{\ln x}{a} + \frac{\ln[h^2 - 1 + (h\mp 1)\sqrt{(h\mp 1)^2 - 4(a^2 \mp h)}\,]}{2a} \\
& \pm \frac{1}{2}\arctan\frac{\sqrt{(h\pm 1)^2 - 4a^2}}{2a}.
\end{aligned}$$

In the particular case when $a = b = 1/4$ we have

$$z = -\frac{y\big(xy + 8 \pm \sqrt{x^2y^2 + 16xy + 60}\,\big)}{2x}$$

and

$$\begin{aligned}
\phi = {} & 2\ln\frac{y}{x} \pm \frac{1}{2}\arctan\frac{1}{\sqrt{4x^2+8x+3}} \\
& \mp 2\ln\big(2 + 2x + \sqrt{4x^2+8x+3}\,\big) \\
& \pm \frac{\sqrt{15}}{2}\operatorname{arctanh}\frac{7+8x}{\sqrt{15(4x^2+8x+3)}},
\end{aligned}$$

see the left part of Fig. 8. On the right side of the same figure one can see the solution of the CAE and orthogonal equiareal pattern obtained when $a = b = 1/10$, $h_{10} = h_{01} = 0$ and $h_{00} = 1$.

Let us note that there is a striking similarity between the spirals in Fig. 8 and spiral fractures actually observed; see, e.g., [52, 53].

Example 4.5.2. Let $b = 0$, $a \neq 0$. This is another case when the integral $E_{a,b}$ can be taken in terms of elementary functions. The pattern is tangent/perpendicular to the equator. The belt spans the parallels $\cos\theta = \pm\sqrt{a^2+1} \mp a$, see Fig. 9(a).

Example 4.5.3. Let $a = 0$, $b \neq 0$, $|b| < \frac{1}{2}$. The pattern has an obvious rotational symmetry; see Figure 9(b). The belt spans the parallels $\cos\theta = \pm\sqrt{1-2b}$.

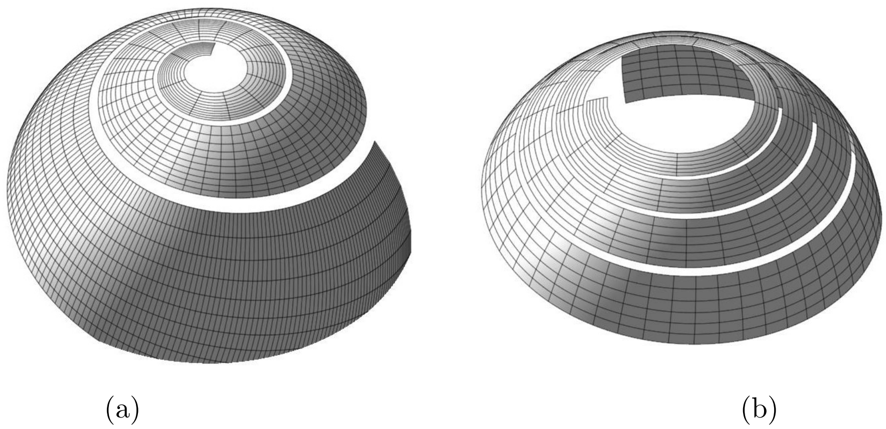

Figure 8: Spherical orthogonal equiareal patterns corresponding to $a = b$; (a) $a = 1/4$, (b) $a = 1/10$.

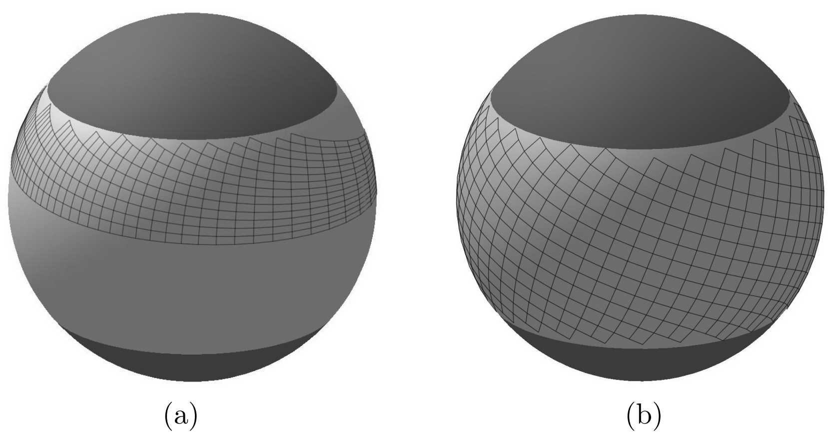

Figure 9: Orthogonal equiareal patterns on the sphere (a) $a = 1/2$, $b = 0$, (b) $a = 0$, $b = 1/3$.

Example 4.5.4. We finish this section providing a picture of slip-line field corresponding to one of the Lipschitz surfaces, see Fig. 10; both branches of a double-valued field are clearly identifiable.

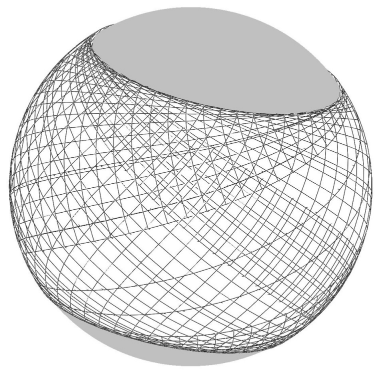

Figure 10: The slip line field on the sphere corresponding to one of the Lipschitz solutions

5 A reciprocal transformation for the CAE

In this section we summarize results from the work [24], where we look for another solution-generating tool that would not require solving differential equations. We introduce two (interrelated) auto-transformations $\mathcal{X}_A$ and $\mathcal{Y}_B$ that, in geometric terms, correspond to taking the involute of the evolute. Each generates a three-parametric family of solutions from a single seed, but when applied in combination, they have an unlimited generating power in terms of the number of arbitrary parameters in the solution.

The transformations $\mathcal{X}_A$ and $\mathcal{Y}_B$ are Bäcklund transformations sensu Bäcklund [4, 19], since each is determined by four relations of no more than the first order (although modern usage often sees this term as implying that independent variables are preserved, the original meaning is as stated). We call $\mathcal{X}_A$ and $\mathcal{Y}_B$ *reciprocal transformations* since, up to point transformations, $\mathcal{X}_A$ and $\mathcal{Y}_B$ are equivalent to $\mathcal{X}$ and $\mathcal{Y}$ satisfying

$$\mathcal{X}^2 = \mathcal{Y}^2 = \mathrm{id},$$

which is a property characteristic of reciprocal transformations [29].

Transformations $\mathcal{X}_A$ and $\mathcal{Y}_B$ only depend on the computation of path-independent line integrals, which puts lower demands on the seeds. The sine-Gordon equation is bypassed and the transformations are immediately applicable to solutions of the constant astigmatism equation with no apriori given sine-Gordon counterpart, such as the Lipschitz solution from the previous section. If the seeds are given in parametric form, then so are the generated solutions.

5.1 First order conservation laws

Firstly, recall the list of symmetries of the CAE from Subsect. 1.3.

We shall also need the six first-order conservation laws of equation (5), which are easy to compute following, e.g., [11]. The associated six potentials $\chi, \mu, \zeta, \tau, \xi, \eta$ satisfy

$$\begin{aligned}
&\chi_x = z_y + y, && \chi_y = \frac{z_x}{z^2} - x, \\
&\mu_x = x z_y, && \mu_y = x\frac{z_x}{z^2} + \frac{1}{z} - x^2, \\
&\zeta_x = -y z_y + z - y^2, && \zeta_y = -y\frac{z_x}{z^2}, \\
&\tau_x = xyz_y - xz + \tfrac{1}{2}\, xy^2, && \tau_y = xy\frac{z_x}{z^2} + \frac{y}{z} - \frac{1}{2}\, x^2 y
\end{aligned} \tag{26}$$

and

$$\begin{aligned}
\xi_x &= \frac{\sqrt{(z_x + z z_y)^2 + 4z^3}}{4z}, & \xi_y &= \frac{\sqrt{(z_x + z z_y)^2 + 4z^3}}{4z^2}, \\
\eta_x &= \frac{\sqrt{(z_x - z z_y)^2 + 4z^3}}{4z}, & \eta_y &= -\frac{\sqrt{(z_x - z z_y)^2 + 4z^3}}{4z^2}.
\end{aligned} \tag{27}$$

Equations (26), (27) are compatible by virtue of equation (5). Potentials ξ, η correspond to the independent variables of the sine-Gordon equation (9), see [5, eq. (29)]. Assuming z positive in accordance to its geometrical meaning (see Def. 3.3.1), the radicands in (27) are positive as well. On the other hand, Manganaro and Pavlov [34] considered the class of solutions such that one of the two radicands is zero.

The involution $\mathfrak{I}$ acts on the potentials as follows: $\mu \longleftrightarrow \zeta$, while $\chi \longrightarrow -\chi$, $\tau \longrightarrow -\tau$, $\xi \longleftrightarrow \xi$, and $\eta \longleftrightarrow -\eta$.

5.2 A geometric construction

Reciprocal transformations results from a construction based on this idea: We start with a constant astigmatism surface $\mathbf{r}$, construct its pseudospherical image $\hat{\mathbf{r}}$, then reconstruct the full preimage $\tilde{\mathbf{r}}$, together with a new solution of the CAE, reflecting the freedom of choice of the parabolic geodesic system on $\hat{\mathbf{r}}$.

Let $z(x, y)$ be a solution of the CAE. The corresponding surface $\mathbf{r}(x, y)$ of constant astigmatism and its unit normal $\mathbf{n}(x, y)$ satisfy the Gauss-Weingarten system (4), which is compatible as a consequence of equation (5).

The family of involutes $\tilde{\mathbf{r}}$ we look for is given by

$$\begin{aligned}\tilde{\mathbf{r}} = \mathbf{r} &+ \Big(\frac{x^2 z \ln z}{x^2 z + 1} + \frac{x^2 z - 1}{x^2 z + 1}(\ln(x^2 z + 1) + a)\Big)\mathbf{n} \\ &+ 2x\frac{2a - 2\ln(x^2 z + 1) + \ln z}{(x^2 z + 1)(2 - \ln z)}\mathbf{r}_x\,,\end{aligned} \tag{28}$$

where a is an arbitrary constant. The corresponding unit normal is

$$\tilde{\mathbf{n}} = \frac{x^2 z - 1}{x^2 z + 1}\mathbf{n} + \frac{4x}{(x^2 z + 1)(2 - \ln z)}\mathbf{r}_x\,. \tag{29}$$

A routine computation shows that the surface $\tilde{\mathbf{r}}(x, y)$ has a constant astigmatism.

However, one more step is required in order to find the corresponding solution of the CAE. Namely, we have to find the adapted curvature coordinates x', y' for the involute. They are

$$x' = b \cdot \frac{xz}{x^2 z + 1} + c_2, \quad y' = \pm\frac{1}{b}\mu + c_3,$$

where μ has been introduced in (26) and b, c_i are constants. Finally,

$$z' = \frac{1}{b^2} \cdot \frac{(x^2 z + 1)^2}{z}.$$

Setting all integration constants c_i to zero, b to 1, and choosing the '+' sign lead us to the following definition of transformations $\mathcal{X}, \mathcal{Y}$.

Definition 5.2.1. Let us define a transformation $\mathcal{X}(x, y, z) = (x', y', z')$ by formulas

$$x' = \frac{xz}{x^2z + 1}, \quad y' = \mu, \quad z' = \frac{(x^2z + 1)^2}{z}. \tag{30}$$

Using $\mathcal{Y} = \mathfrak{I} \circ \mathcal{X} \circ \mathfrak{I}$, we define another transformation $\mathcal{Y}(x, y, z) = (x^*, y^*, z^*)$ by formulas

$$x^* = \zeta, \quad y^* = \frac{y}{y^2 + z}, \quad z^* = \frac{z}{(y^2 + z)^2}. \tag{31}$$

Proposition 5.2.1. *Let $z(x, y)$ be a solution of the constant astigmatism equation* (5)*, ζ, μ the corresponding potentials* (26)*. Let $\mathcal{X}(x, y, z) = (x', y', z')$ and $\mathcal{Y}(x, y, z) = (x^*, y^*, z^*)$ be determined by* (30) *and* (31)*. Then $z'(x', y')$ and $z^*(x^*, y^*)$ are solutions of the constant astigmatism equation* (5) *as well.*

Remark 5.2.1. Note that μ and ζ are potentials defined in (26). Therefore, they are unique up to an integration constant, which is not to be neglected, because it represents a parameter in the solution.

5.3 The reciprocal transformations and their properties

Proposition 5.3.1. *Under a suitable choice of integration constants, $\mathcal{X} \circ \mathcal{X} =$ id and $\mathcal{Y} \circ \mathcal{Y} =$ id.*

Because of this property, $\mathcal{X}$ and $\mathcal{Y}$ are called *reciprocal transformations*, although they are slightly more general than the common reciprocal transformations encountered in the literature, e.g., [29] and [45].

Remark 5.3.1. The transformation $\mathcal{X}$ admits a restriction to the variables x, z and then

$$x'^2 z' = x^2 z, \quad (x'^2 + 1/z')(x^2 + 1/z) = 1,$$

easy to identify with the circle inversion in the $(x, z^{-1/2})$-subspace. Similarly, $\mathcal{Y}$ admits a restriction to the variables y, z, and then

$$y'^2/z' = y^2/z, \quad (y'^2 + z')(y^2 + z) = 1.$$

In this case, we obtain the circle inversion in the $(y, z^{1/2})$-subspace.

The following identities are obvious:

$$\mathcal{X} \circ \mathfrak{I} = \mathfrak{I} \circ \mathcal{Y},$$
$$\mathcal{X} \circ \mathfrak{S}_c = \mathfrak{S}_{1/c} \circ \mathcal{X}, \quad \mathcal{Y} \circ \mathfrak{S}_c = \mathfrak{S}_{1/c} \circ \mathcal{Y}$$

Slightly abusing the notation, we have also

$$\mathcal{X} \circ \mathfrak{T}^y_b = \mathcal{X} = \mathfrak{T}^y_b \circ \mathcal{X},$$
$$\mathcal{Y} \circ \mathfrak{T}^x_a = \mathcal{Y} = \mathfrak{T}^x_a \circ \mathcal{Y}.$$

There is no similar identity for $\mathcal{X} \circ \mathfrak{T}^x_a$ and $\mathcal{Y} \circ \mathfrak{T}^y_b$. Instead, $\mathcal{X}, \mathfrak{T}^x_a$ generate a three-parameter group, and so do $\mathcal{Y}, \mathfrak{T}^y_b$.

Proposition 5.3.2. *Let $z(x, y)$ be a solution of the constant astigmatism equation* (5)*, χ, μ, ζ the corresponding potentials* (26)*, and*

$$A = \begin{pmatrix} a_{11} & a_{12} \\ a_{21} & a_{22} \end{pmatrix} \tag{32}$$

a real matrix such that $\det A = \pm 1$. Let $\mathcal{X}_A(x, y, z) = (x'_A, y'_A, z'_A)$ and $\mathcal{Y}_A(x, y, z) = (x^*_A, y^*_A, z^*_A)$, where

$$x'_A = \frac{(a_{11} + a_{12}x)(a_{21} + a_{22}x)z + a_{12}a_{22}}{(a_{11} + a_{12}x)^2 z + a_{12}^2},$$
$$\pm y'_A = a_{12}^2 \mu + a_{11}a_{12}\chi - a_{11}y(a_{11} + a_{12}x),$$
$$z'_A = \frac{((a_{11} + a_{12}x)^2 z + a_{12}^2)^2}{z}$$

and

$$\pm x^*_A = a_{12}^2 \zeta - a_{11}a_{12}\chi - a_{11}x(a_{11} + a_{12}y),$$
$$y^*_A = \frac{(a_{11} + a_{12}y)(a_{21} + a_{22}y) + a_{12}a_{22}z}{(a_{11} + a_{12}y)^2 + a_{12}^2 z},$$
$$z^*_A = \frac{z}{((a_{11} + a_{12}y)^2 + a_{12}^2 z)^2}$$

Then $z'_A(x'_A, y'_A)$ and $z^*_A(x^*_A, y^*_A)$ are solutions of the constant astigmatism equation (5) *as well. The corresponding surfaces* (28) *exhaust all constant astigmatism surfaces sharing one of the evolutes with the seed surface* $\mathbf{r}$.

The Lie symmetries established in Subsect. 1.3 correspond to $\mathcal{X}_A$ according to the following table:

Lie symmetry	$\mathfrak{T}^x_a$	$\mathfrak{S}_c$	$\mathcal{X}$
matrix A	$\begin{pmatrix} \mathrm{i} & 0 \\ a\mathrm{i} & \mathrm{i} \end{pmatrix}$	$\begin{pmatrix} \sqrt{c} & 0 \\ 0 & 1/\sqrt{c} \end{pmatrix}$	$\begin{pmatrix} 0 & 1 \\ 1 & 0 \end{pmatrix}$.

Recall that the translation $\mathfrak{T}^y_a$ is due to the non-uniqueness of μ; see Remark 5.2.1. Otherwise said, $\mathfrak{T}^y_a$ corresponds to the unit matrix.

Proposition 5.3.3. *In the case when $a_{12} = 0$ the transformations reduce to local symmetries*

$$\mathcal{X}_A = \begin{cases} \mathfrak{T}^x_{a_{21}/a_{11}} \circ \mathfrak{S}_{-a_{11}^2} & \text{if } \det A = -1, \\ \mathfrak{T}^x_{a_{21}/a_{11}} \circ \mathcal{R}^y \circ \mathfrak{S}_{-a_{11}^2} & \text{if } \det A = +1, \end{cases}$$

$$\mathcal{Y}_A = \begin{cases} \mathfrak{T}^y_{a_{21}/a_{11}} \circ \mathfrak{S}_{-1/a_{11}^2} & \text{if } \det A = -1, \\ \mathfrak{T}^y_{a_{21}/a_{11}} \circ \mathcal{R}^x \circ \mathfrak{S}_{-1/a_{11}^2} & \text{if } \det A = +1. \end{cases}$$

Proposition 5.3.4. *We have*

$$\mathcal{X}_B \circ \mathcal{X}_A = \mathcal{X}_{BA}, \quad \mathcal{Y}_B \circ \mathcal{Y}_A = \mathcal{Y}_{BA}$$

for any two 2×2 matrices A, B such that $|\det A| = |\det B| = 1$.

It follows that transformations $\mathcal{X}_A$ form a three-parameter group, and similarly for the transformations $\mathcal{Y}_A$.

5.4 Relation to the sine-Gordon equation

Let us discuss the reciprocal transformation in terms of the sine-Gordon solutions. It is closely related to the Bäcklund relation $\mathcal{B}^{(\lambda)}$, given by the system (10). It follows that, on the level of sine-Gordon solutions, alternate repeating of transformations $\mathcal{X}_A$ and $\mathcal{Y}_B$ corresponds to alternate repeating the Bäcklund transformation with Bäcklund parameter $\lambda = \pm 1$ according to a commutative diagram

$$\begin{tikzcd}
\bullet \arrow[rr, "\mathcal{X}_A"] \arrow[dr, "\mathcal{F}_1"'] & & \bullet \arrow[rr, "\mathcal{Y}_B"] \arrow[dl, "\mathcal{F}_1"] \arrow[dr, "\mathcal{F}_2"'] & & \bullet \arrow[rr, "\mathcal{X}_A"] \arrow[dl, "\mathcal{F}_2"] \arrow[dr, "\mathcal{F}_1"'] & & \bullet \arrow[rr, "\mathcal{Y}_B"] \arrow[dl, "\mathcal{F}_1"] \arrow[dr, "\mathcal{F}_2"'] & & \bullet \arrow[dl, "\mathcal{F}_2"] \arrow[dr, "\mathcal{F}_1"'] & \\
& \bullet \arrow[rr, "\mathcal{B}^{(1)}"'] & & \bullet \arrow[rr, "\mathcal{B}^{(-1)}"'] & & \bullet \arrow[rr, "\mathcal{B}^{(1)}"'] & & \bullet \arrow[rr, "\mathcal{B}^{(-1)}"'] & & \bullet
\end{tikzcd}$$

easily extensible to the left or to the right. In the diagram, the mappings $\mathcal{F}_i(x, y, z) = (\xi, \eta, \omega_i)$ from the CAE to the sine-Gordon equation are so called *focal mappings*. They map solutions $z(x, y)$ of the CAE to two complementary sine-Gordon solutions $\omega_1(\xi, \eta), \omega_2(\xi, \eta)$ given by formulas [24, p. 12]

$$\omega_1 = \arctan \frac{4z^{3/2} z_x}{z_x^2 - 4z^3 - z^2 z_y^2} \quad \text{and} \quad \omega_2 = \arctan \frac{4z^{5/2} z_y}{z_x^2 + 4z^3 - z^2 z_y^2}.$$

5.5 Transformation of orthogonal equiareal patterns and constant astigmatism surfaces

The Gaussian image, $\tilde{\mathbf{n}}$, of the transformed surface is given by formula (29). It is easily checked that the first fundamental form of $\tilde{\mathbf{n}}$ in terms of coordinates x', y' defined by (30) is

$$\mathbf{I}_{\tilde{\mathbf{n}}} = z'(\mathrm{d}x')^2 + \frac{1}{z'}(\mathrm{d}y')^2$$

and therefore generates a new orthogonal equiareal pattern on the transformed surface's Gaussian sphere.

What is the relationship between the initial and the transformed pattern? Let ψ denote the angle between $\mathbf{n}$ and $\tilde{\mathbf{n}}$. Then

$$\tilde{\mathbf{n}} = \cos\psi\, \mathbf{n} + \sin\psi \frac{\mathbf{n}_x}{\sqrt{z}},$$

where $\mathbf{n}_x/\sqrt{z}$ is the unit vector codirectional with $\mathbf{n}_x$.

The vectors tangent to the lines $y' = \text{const}$ and $x' = \text{const}$ at the point $\tilde{\mathbf{n}}(x, y)$ are

$$\tilde{\mathbf{n}}_{x'} = \frac{x^2 z - 1}{z}\mathbf{n}_x - 2x\mathbf{n}, \qquad \tilde{\mathbf{n}}_{y'} = -\frac{z}{x^2 z + 1}\mathbf{n}_y.$$

Consequently, $\mathbf{n}, \mathbf{n}_x, \tilde{\mathbf{n}}$ and $\tilde{\mathbf{n}}_{x'}$ lie in one and the same plane, while $\mathbf{n}_y$ and $\tilde{\mathbf{n}}_{y'}$ are orthogonal to it. The angle between $\tilde{\mathbf{n}}_{x'}$ and $\mathbf{n}_x$ is ψ.

The transformed orthogonal equiareal pattern can be constructed in the following way: Rotate the vector $\mathbf{n}$ by angle ψ in the plane spanned by $\mathbf{n}$ and $\mathbf{n}_x$. One of the new tangent vectors, $\tilde{\mathbf{n}}_{x'}$, lies in the above-mentioned plane while the second one, $\tilde{\mathbf{n}}_{y'}$, is orthogonal to it. Figure 11 provides a schematic picture of the construction.

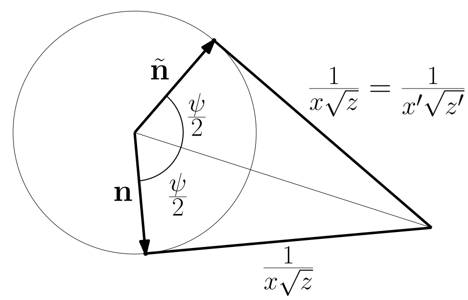

Figure 11: The transformation of an orthogonal equiareal pattern. Intersection of the Gaussian sphere with the plane containing $\mathbf{n}, \mathbf{n}_x, \tilde{\mathbf{n}}, \tilde{\mathbf{n}}_{x'}$.

Similarly, formula (28), which describes the reciprocal transformation in terms of constant astigmatism surfaces, can be rewritten simply as

$$\tilde{\mathbf{r}} = \mathbf{r} + (\rho_2 - \rho_2' \cos\psi)\,\mathbf{n} - \rho_2' \sin\psi\,\mathbf{e}\,, \tag{33}$$

where ρ_2 was established in (3), ρ_2' (one of the transformed surface's radii of curvature) is given by

$$\rho_2' = \ln \frac{\sqrt{z}}{x^2 z + 1} + a$$

and $\mathbf{e} = -\mathbf{r}_x/u$ is a unit vector codirectional or contradirectional (depending on the value of z) with $\mathbf{r}_x$. Here a denotes the same constant as in (28).

5.6 Examples

Example 5.6.1. Let us apply the transformations $\mathcal{X}$ and $\mathcal{Y}$ to the von Lilienthal solution (cf. (6))

$$z = b^2 - y^2,$$

where b is a constant.

Using (30), we obtain $\mathcal{X}(x,y,z) = (x',y',z')$, where

$$
\begin{aligned}
x' &= \frac{x(b^2-y^2)}{x^2(b^2-y^2)+1}\,, \\
y' &= \mu = \frac{1}{b}\operatorname{arctanh}\Big(\frac{y}{b}\Big) - x^2 y + c_1\,, \\
z' &= \frac{(x^2(b^2-y^2)+1)^2}{b^2-y^2},
\end{aligned}
\tag{34}
$$

c_1 being the integration constant. Here μ has been expressed as a line integral according to formula (26). Apparently, $z'(x',y')$ is a substantially new solution of the CAE.

Similarly, using (31), we obtain $\mathcal{Y}(x,y,z) = (x^*,y^*,z^*)$, where

$$
x^* = b^2 x + c_2\,, \quad y^* = \frac{y}{b^2}\,, \quad z^* = \frac{b^2-y^2}{b^4}. \tag{35}
$$

However, $z^* = -{y^*}^2 + 1/b^2$ and, thus, we obtained just another von Lilienthal solution.

Remark 5.6.1. Examples in this section demonstrate that reciprocal transformations inevitably produce solutions in parametric form. While inconvenient, this is not a serious obstacle. Both iteration of the procedure and construction of the constant astigmatism surface or the orthogonal equiareal pattern are possible. However, it is not straightforward to see whether two solutions coincide up to a reparameterisation.

Example 5.6.2. Continuing Example 5.6.1, we provide a picture of the surface of constant astigmatism generated from the von Lilienthal seed. It is given by formula

$$
\begin{aligned}
\tilde{\mathbf{r}}_1 &= \gamma(b,x,y)\{2b\sin(bx) - [x^2(b^2-y^2)-1]\cos(bx)\}, \\
\tilde{\mathbf{r}}_2 &= -\gamma(b,x,y)\{2b\cos(bx) + [x^2(b^2-y^2)-1]\sin(bx)\}, \\
\tilde{\mathbf{r}}_3 &= \frac{x^2(b^2-y^2)-1}{x^2(b^2-y^2)+1}\, y\ln[x^2(b^2-y^2)+1] \\
&\quad + \frac{b+y}{2b}\cdot\frac{x^2(b-y)^2+1}{x^2(b^2-y^2)+1}\, y\ln(b^2-y^2) - \ln(b-y) - \frac{y}{b},
\end{aligned}
$$

where

$$\gamma(b,x,y) = \frac{\sqrt{b^2-y^2}}{2b} \cdot \frac{x^2(b^2-y^2)+1}{2\ln[x^2(b^2-y^2)+1] - \ln(b^2-y^2)+1}.$$

Obviously, $\tilde{\mathbf{r}}$ is real only if $-b < y < b$. A part of the surface is shown in Figure 12 under the parameterisation by x, y. To parameterise the surface by lines of curvature, one would have to express x, y in terms of x', y' from formula (34).

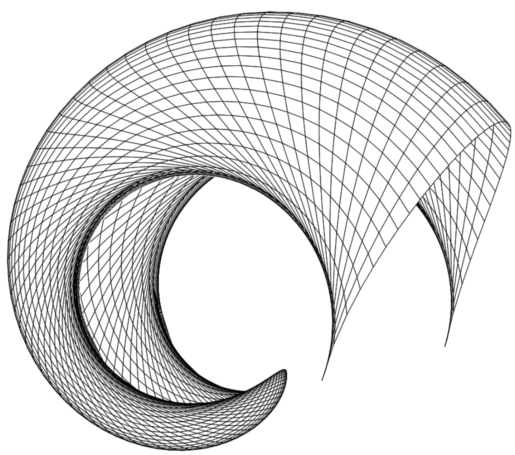

Figure 12: A transformed von Lilienthal surface.

Example 5.6.3. Continuing previous example we describe the transformation of the corresponding orthogonal equiareal pattern. The von Lilienthal solution $z = b^2 - y^2$ generates the Archimedean projection (see Example 3.1.1)

$$\mathbf{I}_{\text{Arch}} = (b^2 - y^2)\,\mathrm{d}x^2 + \frac{1}{b^2-y^2}\,\mathrm{d}y^2.$$

The Gaussian image of the transformed surface is

$$
\begin{aligned}
\tilde{\mathbf{n}}_1 &= \frac{\sqrt{b^2-y^2}}{b} \cdot \frac{(x^2(b^2-y^2)-1)\cos(bx) - 2xb\sin(bx)}{x^2(b^2-y^2)+1}, \\
\tilde{\mathbf{n}}_2 &= \frac{\sqrt{b^2-y^2}}{b} \cdot \frac{(x^2(b^2-y^2)-1)\sin(bx) + 2xb\cos(bx)}{x^2(b^2-y^2)+1}, \\
\tilde{\mathbf{n}}_3 &= -\frac{y}{b} \cdot \frac{x^2(b^2-y^2)-1}{x^2(b^2-y^2)+1}.
\end{aligned}
\tag{36}
$$

To express the $\mathcal{X}$-transformed orthogonal equiareal pattern explicitly, one needs to invert the transformation $(x, y) \leftrightarrow (x', y')$, where x', y' are given by formula (34). The $\mathcal{X}$-transformed orthogonal equiareal pattern $\tilde{\mathbf{n}}'(x', y')$ can be seen in the right part of Figure 13.

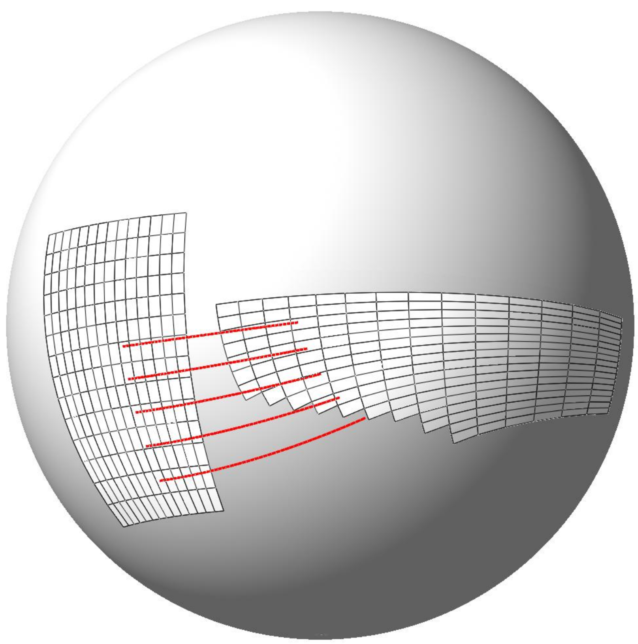

Figure 13: A part of Archimedean projection (left) and a part of its $\mathcal{X}$-transformed pattern (right) connected by great circles' arcs.

6 Nonlocal conservation laws of the CAE

This section is devoted to summarizing results from the work [26].

Potentials ζ, μ from (26) are images of x, y under the reciprocal transformations $\mathcal{Y}, \mathcal{X}$, respectively; see formulas (30), (31). Applying $\mathcal{X}$ to ζ and $\mathcal{Y}$ to μ, we obtain new nonlocal potentials and the process can be continued indefinitely. It is then natural to ask what is the minimal set of potentials closed under the action of $\mathcal{X}$ and $\mathcal{Y}$.

6.1 Conservation laws

Let $\mathcal{E}$ be a system of partial differential equations in two independent variables x, y. A conservation law is a 1-form $f\,\mathrm{d}x + g\,\mathrm{d}y$ such that $f_y - g_x = 0$ as a consequence of the system $\mathcal{E}$. A *potential*, say ϕ, corresponding to this conservation law is a variable which formally satisfies the compatible system $\phi_y = f$, $\phi_x = g$.

Let $\mathfrak{g}$ be a matrix Lie algebra. A $\mathfrak{g}$-valued zero curvature representation [55] of the system $\mathcal{E}$ is a 1-parametric family $\mathfrak{g}$-valued forms $\alpha(\lambda) = A(\lambda)\,\mathrm{d}x + B(\lambda)\,\mathrm{d}y$ such that $A_y - B_x + [A, B] = 0$ as a consequence of the system $\mathcal{E}$.

Let Q be an arbitrary matrix (called a *gauge matrix*) belonging to the associated Lie group $\mathcal{G}$. The *gauge transformation* [55] with respect to Q sends $\alpha = A\,\mathrm{d}x + B\,\mathrm{d}y$ to ${}^Q\alpha = {}^QA\,\mathrm{d}x + {}^QB\,\mathrm{d}y$, where

$$ {}^QA = Q_xQ^{-1} + QAQ^{-1}, \quad {}^QB = Q_yQ^{-1} + QBQ^{-1}. \tag{37}$$

We also say that ${}^QA, {}^QB$ are *gauge equivalent* to A, B.

Let us explain the procedure to generate conservation laws. Undoubtedly, the shortest way to conservation laws is from a zero curvature representation that vanishes at some value λ_0 of λ. Without loss of generality we assume that $\lambda_0 = 0$, i.e., $A(0) = B(0) = 0$. Consider the associated compatible linear system [55] (or a differential covering [11, 30])

$$\Phi_x = A\Phi, \quad \Phi_y = B\Phi, \tag{38}$$

where Φ is a column vector. Expanding Φ into the formal power series

$$\Phi = \sum_{i=0}^{\infty} \Phi_i \lambda^i$$

around zero and inserting into (38), we obtain compatible equations

$$\Phi_{n,x} = \sum_{i=1}^{n} A_i \Phi_{n-i}, \quad \Phi_{n,y} = \sum_{i=1}^{n} B_i \Phi_{n-i}, \quad n \geq 0, \tag{39}$$

where A_i, B_i are the coefficients of the Taylor expansion of A, B around $\lambda = 0$. Here we start from $i = 1$ since $A_0 = B_0 = 0$. By formulas (39), each of the derivatives $\Phi_{n,x}, \Phi_{n,y}$ is explicitly expressed in terms of $\Phi_0, \ldots, \Phi_{n-1}$. Moreover, $\Phi_{0,x} = \Phi_{0,y} = 0$, meaning that Φ_0 is a constant vector. Choosing Φ_0 suitably, we can subsequently use equations (39) to express the derivatives $\Phi_{n,x}, \Phi_{n,y}$ in terms of the previously determined potentials Φ_i, $i < n$, obtaining what may be called a hierarchy of vectorial potentials determined by $\Phi_0 = \text{const} \neq 0$ and

$$\begin{aligned}
\Phi_{1,x} &= A_1 \Phi_0, & \Phi_{1,y} &= B_1 \Phi_0, \\
\Phi_{2,x} &= A_1 \Phi_1 + A_2 \Phi_0, & \Phi_{2,y} &= B_1 \Phi_1 + B_2 \Phi_0, \\
\Phi_{3,x} &= A_1 \Phi_2 + A_2 \Phi_1 + A_3 \Phi_0, & \Phi_{3,y} &= B_1 \Phi_2 + B_2 \Phi_1 + B_3 \Phi_0, \\
&\vdots
\end{aligned}$$

The 1-forms

$$\sum_{i=1}^{n} A_i \Phi_{n-i} \, \mathrm{d}x + \sum_{i=1}^{n} B_i \Phi_{n-i} \, \mathrm{d}y$$

then constitute a hierarchy of vectorial conservation laws, linear in the potentials Φ_i. Their components are the scalar conservation laws sought. They are termed 'nonlocal' since they depend on the potentials. The whole hierarchy of potentials is also a special abelian covering [11].

As is well known, linearly independent conservation laws can have functionally dependent potentials; cf. the discussion of local or potential dependence in [43].

6.2 The zero curvature representation

From now on, we deal with the constant astigmatism equation (5).

The zero curvature representation $\alpha = A(\lambda)\,\mathrm{d}x + B(\lambda)\,\mathrm{d}y$ satisfying the assumption $A(0) = B(0) = 0$ is

$$
\begin{aligned}
A(\lambda) &= \begin{pmatrix} \dfrac{\lambda(\lambda-2)K_1}{2(\lambda-1)} - \dfrac{\lambda^2 z L_1}{2(\lambda-1)} & \dfrac{\lambda^2 z}{4(\lambda-1)} \\ \dfrac{\lambda(\lambda-2)K_2}{2(\lambda-1)} - \dfrac{\lambda^2 z L_2}{2(\lambda-1)} & -\dfrac{\lambda(\lambda-2)K_1}{2(\lambda-1)} + \dfrac{\lambda^2 z L_1}{2(\lambda-1)} \end{pmatrix}, \\
B(\lambda) &= \begin{pmatrix} \dfrac{\lambda(\lambda-2)L_1}{2(\lambda-1)} - \dfrac{\lambda^2 K_1}{2(\lambda-1)z} & -\dfrac{\lambda(\lambda-2)}{4(\lambda-1)} \\ \dfrac{\lambda(\lambda-2)L_2}{2(\lambda-1)} - \dfrac{\lambda^2 K_2}{2(\lambda-1)z} & -\dfrac{\lambda(\lambda-2)L_1}{2(\lambda-1)} + \dfrac{\lambda^2 K_1}{2(\lambda-1)z} \end{pmatrix},
\end{aligned}
\tag{40}
$$

where

$$
\begin{aligned}
K_1 &= -\frac{z_y}{4}, \qquad L_1 = -\frac{z_x}{4z^2} + \frac{x}{2}, \\
K_2 &= -\frac{x z_y}{2}, \quad L_2 = -\frac{x z_x}{2z^2} - \frac{1}{2z} + \frac{x^2}{2}.
\end{aligned}
\tag{41}
$$

Thus, we can derive a double hierarchy of nonlocal conservation laws by expansion of a 2-component vector Φ satisfying system (38), i.e.,

$$
\Phi_x = A\Phi, \quad \Phi_y = B\Phi. \tag{42}
$$

Before doing that, consider the transformation properties of these hierarchies under local and nonlocal symmetries. As the initial step we transform the zero curvature representation itself.

To start with, the CAE is invariant under the duality (7), in this section denoted by

$$
\bar{x} = y, \quad \bar{y} = x, \quad \bar{z} = \frac{1}{z}.
$$

By applying duality to the zero curvature representation $A\,\mathrm{d}x + B\,\mathrm{d}y$, we obtain $\bar{A}\,\mathrm{d}\bar{x} + \bar{B}\,\mathrm{d}\bar{y} = \bar{B}\,\mathrm{d}x + \bar{A}\,\mathrm{d}y$, where $\bar{A}, \bar{B}$ result from A, B by replacing K_i, L_i with

$$
\begin{aligned}
\bar{K}_1 &= \frac{z_x}{4z^2}, \quad \bar{L}_1 = \frac{z_y}{4} + \frac{y}{2}, \\
\bar{K}_2 &= \frac{y z_x}{2z^2}, \quad \bar{L}_2 = \frac{y z_y}{2} - \frac{z}{2} + \frac{y^2}{2}.
\end{aligned}
\tag{43}
$$

Thus, the *dual conservation laws* will be derived by expansion of $\bar{\Phi}$ satisfying the system

$$\bar{\Phi}_x = \bar{B}\bar{\Phi}, \quad \bar{\Phi}_y = \bar{A}\bar{\Phi}. \tag{44}$$

Furthermore, the CAE is invariant under the reciprocal transformations $\mathcal{X}(x, y, z) = (\tilde{x}, \tilde{y}, \tilde{z})$ and $\mathcal{Y}(x, y, z) = (x^*, y^*, z^*)$, see Def. 5.2.1 from the previous section. Since $\mathcal{X}$ is related to $\mathcal{Y}$ by the duality (7), we shall focus on one of them, namely $\mathcal{X}$.

The image of the zero curvature representation $A\,\mathrm{d}x + B\,\mathrm{d}y$ under $\mathcal{X}$ is $A'\,\mathrm{d}x' + B'\,\mathrm{d}y' = \widetilde{A}\,\mathrm{d}x + \widetilde{B}\,\mathrm{d}y$, where

$$\widetilde{A}(\lambda) = \begin{pmatrix} -\dfrac{\lambda(\lambda-2)K_1}{2(\lambda-1)} + \dfrac{\lambda^2 z L_1}{2(\lambda-1)} & \dfrac{\lambda(\lambda-2)K_2}{2(\lambda-1)} - \dfrac{\lambda^2 z L_2}{2(\lambda-1)} \\ \dfrac{\lambda^2 z}{4(\lambda-1)} & \dfrac{\lambda(\lambda-2)K_1}{2(\lambda-1)} - \dfrac{\lambda^2 z L_1}{2(\lambda-1)} \end{pmatrix},$$

$$\widetilde{B}(\lambda) = \begin{pmatrix} -\dfrac{\lambda(\lambda-2)L_1}{2(\lambda-1)} + \dfrac{\lambda^2 K_1}{2(\lambda-1)z} & \dfrac{\lambda(\lambda-2)L_2}{2(\lambda-1)} - \dfrac{\lambda^2 K_2}{2(\lambda-1)z} \\ -\dfrac{\lambda(\lambda-2)}{4(\lambda-1)} & \dfrac{\lambda(\lambda-2)L_1}{2(\lambda-1)} - \dfrac{\lambda^2 K_1}{2(\lambda-1)z} \end{pmatrix},$$

with K_i, L_i being given by formulas (41). Thus, the *reciprocal conservation laws* will be derived by expansion of Φ' satisfying the system

$$\Phi'_x = \widetilde{A}\Phi', \quad \Phi'_y = \widetilde{B}\Phi'. \tag{45}$$

Finally, *reciprocal dual conservation laws* are derived from $\bar{A}'\,\mathrm{d}\bar{x}' + \bar{B}'\,\mathrm{d}\bar{y}'$.

6.3 The hierarchies

Denote

$$\Phi = \begin{pmatrix} u \\ v \end{pmatrix}, \quad \bar{\Phi} = \begin{pmatrix} \bar{u} \\ \bar{v} \end{pmatrix}, \quad \Phi' = \begin{pmatrix} u' \\ v' \end{pmatrix}, \quad \bar{\Phi}' = \begin{pmatrix} \bar{u}' \\ \bar{v}' \end{pmatrix}$$

the vectors generating ordinary, dual, reciprocal, and reciprocal dual hierarchy of nonlocal conservation laws, respectively.

Construction 1. *Denote*

$$u_0 = 1, \qquad v_0 = 0,$$

and define potentials u_n, v_n by induction

$$\begin{aligned}
u_{n,x} &= K_1 u_{n-1} + \frac{1}{2}\,(K_1 + zL_1) \sum_{i=0}^{n-2} u_i - \frac{1}{4}\, z \sum_{i=0}^{n-2} v_i, \\
u_{n,y} &= L_1 u_{n-1} - \frac{1}{2}\, v_{n-1} + \frac{1}{2}\left(L_1 + \frac{K_1}{z}\right) \sum_{i=0}^{n-2} u_i - \frac{1}{4} \sum_{i=0}^{n-2} v_i, \\
v_{n,x} &= K_2 u_{n-1} - K_1 v_{n-1} + \frac{1}{2}\,(K_2 + zL_2) \sum_{i=0}^{n-2} u_i - \frac{1}{2}\,(K_1 + zL_1) \sum_{i=0}^{n-2} v_i, \\
v_{n,y} &= L_2 u_{n-1} - L_1 v_{n-1} + \frac{1}{2}\left(L_2 + \frac{K_2}{z}\right) \sum_{i=0}^{n-2} u_i - \frac{1}{2}\left(L_1 + \frac{K_1}{z}\right) \sum_{i=0}^{n-2} v_i,
\end{aligned} \tag{46}$$

for all $n > 0$, with K_1, K_2, L_1, L_2 being as introduced by formulas (41) *above.*

By construction, u_i, v_i are potentials of nonlocal conservation laws of the constant astigmatism equation. Observe that $u_{1,x} = K_1$, $u_{1,y} = L_1$, $v_{1,x} = K_2$, $v_{1,y} = L_2$ are local. As we shall see later, the potentials u_n, v_n are mutually independent. Choosing a different initial vector $\Phi_0 \neq 0$, one obtains another set of potentials, linearly dependent on the potentials just constructed.

The constant astigmatism equation is invariant under the duality (7), while Construction 1 is not. Mutatis mutandis, we obtain the dual construction.

Construction 2. *Denote*

$$\bar{u}_0 = 1, \qquad \bar{v}_0 = 0,$$

and define potentials $\bar{u}_n, \bar{v}_n$ *by induction*

$$\begin{aligned}
\bar{u}_{n,x} &= \bar{L}_1 \bar{u}_{n-1} - \frac{1}{2}\,\bar{v}_{n-1} + \frac{1}{2}\,(\bar{L}_1 + z\bar{K}_1) \sum_{i=0}^{n-2} \bar{u}_i - \frac{1}{4} \sum_{i=0}^{n-2} \bar{v}_i, \\
\bar{u}_{n,y} &= \bar{K}_1 \bar{u}_{n-1} + \frac{1}{2}\left(\bar{K}_1 + \frac{\bar{L}_1}{z}\right) \sum_{i=0}^{n-2} \bar{u}_i - \frac{1}{4z} \sum_{i=0}^{n-2} \bar{v}_i, \\
\bar{v}_{n,x} &= \bar{L}_2 \bar{u}_{n-1} - \bar{L}_1 \bar{v}_{n-1} + \frac{1}{2}\,(\bar{L}_2 + z\bar{K}_2) \sum_{i=0}^{n-2} \bar{u}_i - \frac{1}{2}\,(\bar{L}_1 + z\bar{K}_1) \sum_{i=0}^{n-2} \bar{v}_i, \\
\bar{v}_{n,y} &= \bar{K}_2 \bar{u}_{n-1} - \bar{K}_1 \bar{v}_{n-1} + \frac{1}{2}\left(\bar{K}_2 + \frac{\bar{L}_2}{z}\right) \sum_{i=0}^{n-2} \bar{u}_i - \frac{1}{2}\left(\bar{K}_1 + \frac{\bar{L}_1}{z}\right) \sum_{i=0}^{n-2} \bar{v}_i,
\end{aligned} \tag{47}$$

for all $n > 0$*, with* $\bar{K}_1, \bar{K}_2, \bar{L}_1, \bar{L}_2$ *being given by formulas* (43) *above.*

By construction, $\bar{u}_i, \bar{v}_i$ are also nonlocal potentials of the constant astigmatism equation. They are said to be dual to u_i, v_i. However, $u_i, v_i, \bar{u}_i, \bar{v}_i$ are not functionally independent, as we shall see below. We shall not present any construction of potentials $u'_i, v'_i, \bar{u}'_i, \bar{v}'_i$. Instead, in the next subsection, we shall show how they depend on the potentials $u_i, v_i, \bar{u}_i, \bar{v}_i$ already constructed.

Remark 6.3.1. The potentials χ, ζ, μ, τ introduced in (26) are functions of x, y, z, u_1, v_1, $w_1 = \bar{v}_1$, namely

$$\begin{aligned}
\mu &= -2v_1, & \chi &= -4u_1 + xy, \\
\zeta &= -2w_1, & \tau &= 2u_1^2 + 2u_1 - 4u_2 - 2yv_1 - \tfrac{1}{2}\ln z + \tfrac{1}{4}\,x^2 y^2.
\end{aligned}$$

6.4 Relations between potentials

The reciprocal and reciprocal dual conservation laws depend on ordinary and dual conservation laws according to following two propositions.

Proposition 6.4.1. *Potentials u_i, v_i, $\bar{u}_i$, $\bar{v}_i$ transform under $\mathcal{X}$ as follows:*

$$u_i' = \bar{u}_i - \frac{1}{2}\,(1+xy)\bar{u}_{i-1} + \frac{1}{2}\,x\bar{v}_{i-1},$$

$$v_i' = -\frac{1}{2}\,y\bar{u}_{i-1} + \frac{1}{2}\,\bar{v}_{i-1},$$

$$\bar{u}_i' = \sum_{j=0}^{i} \frac{1}{2^{i-j}}\Big(u_j - \frac{xz}{x^2z+1}v_j\Big),$$

$$\bar{v}_i' = 2v_{i+1} - 2v_1 \sum_{j=0}^{i} \frac{1}{2^{i-j}}\Big(u_j - \frac{xz}{x^2z+1}v_j\Big).$$

Moreover, $p_i'' = p$ for each potential $p_i = u_i, v_i, \bar{u}_i, \bar{v}_i$.

Proposition 6.4.2. *Potentials u_i, v_i, $\bar{u}_i$, $\bar{v}_i$ transform under $\mathcal{Y}$ as follows:*

$$u_i^* = \sum_{j=0}^{i} \frac{1}{2^{i-j}}\Big(\bar{u}_j - \frac{y}{y^2+z}\bar{v}_j\Big),$$

$$v_i^* = 2v_{i+1} - 2\bar{v}_1 \sum_{j=0}^{i} \frac{1}{2^{i-j}}\Big(\bar{u}_j - \frac{y}{y^2+z}\bar{v}_j\Big),$$

$$\bar{u}_i^* = u_i - \frac{1}{2}\,(1+xy)u_{i-1} + \frac{1}{2}\,yv_{i-1},$$

$$\bar{v}_i^* = -\frac{1}{2}\,xu_{i-1} + \frac{1}{2}\,v_{i-1}.$$

Moreover, $p_i^{**} = p$ for each potential $p_i = u_i, v_i, \bar{u}_i, \bar{v}_i$.

We see that equalities $\mathcal{X} \circ \mathcal{X} = \mathrm{id} = \mathcal{Y} \circ \mathcal{Y}$ still hold after extension of $\mathcal{X}, \mathcal{Y}$ to the higher potentials.

Since reciprocal and reciprocal dual conservation laws are linear combinations of on ordinary and dual conservation laws, we focus on the latter, i.e. u_i, v_i and $\bar{u}_i, \bar{v}_i$. It follows that hierarchies u_i, v_i, $\bar{u}_i, \bar{v}_i$ are not independent.

Proposition 6.4.3. *For all integers $n \geq -1$ and constants c_i, we have the relations*

$$\begin{aligned}\sum_{i=0}^{n} u_i \bar{u}_{n-i} + \sum_{i=0}^{n} (x u_i - v_i)(y \bar{u}_{n-i} - \bar{v}_{n-i}) \\ - 2 \sum_{i=0}^{n+1} u_i \bar{u}_{n-i+1} - c_{n+1} = 0.\end{aligned} \tag{48}$$

We have the freedom to choose $c(\lambda) \neq 0$ (if $c = 0$, then the three hierarchies are functionally dependent again). To have $\bar{u}_0 = 1$, we choose $c = -2$, i.e., $c_0 = -2$, $c_i = 0$ for $i > 0$. Solving (48) with respect to $\bar{u}_{k+1}$ and renaming $\bar{v}_i$ to w_i, we get the recursion formulas

$$\begin{aligned}\bar{u}_0 &= 1, \\ \bar{u}_{k+1} &= \frac{1 + xy}{2} \sum_{i=0}^{k} u_i \bar{u}_{k-i} - \frac{y}{2} \sum_{i=0}^{k} \bar{u}_i v_{k-i} + \frac{1}{2} \sum_{i=0}^{k} (v_i - x u_i) w_{k-i} \\ &\quad - \sum_{i=1}^{k+1} u_i \bar{u}_{k-i+1}.\end{aligned} \tag{49}$$

E.g., $\bar{u}_1 = -u_1 + \frac{1}{2}(1 + xy)$, etc.

Assuming assignments (49) and denoting $w_i = \bar{v}_i$, systems (46) and (47) reduce to covering (50) below.

Construction 3. *Let*

$$u_0 = 1, \qquad v_0 = w_0 = 0,$$

and define potentials u_n, v_n, w_n *by induction*

$$\begin{aligned}
u_{n,x} &= K_1 u_{n-1} + \frac{1}{2}(K_1 + zL_1)\sum_{i=0}^{n-2} u_i - \frac{1}{4}\, z \sum_{i=0}^{n-2} v_i, \\
u_{n,y} &= L_1 u_{n-1} - \frac{1}{2}\, v_{n-1} + \frac{1}{2}\left(L_1 + \frac{K_1}{z}\right)\sum_{i=0}^{n-2} u_i - \frac{1}{4}\sum_{i=0}^{n-2} v_i, \\
v_{n,x} &= K_2 u_{n-1} - K_1 v_{n-1} + \frac{1}{2}(K_2 + zL_2)\sum_{i=0}^{n-2} u_i - \frac{1}{2}(K_1 + zL_1)\sum_{i=0}^{n-2} v_i, \\
v_{n,y} &= L_2 u_{n-1} - L_1 v_{n-1} + \frac{1}{2}\left(L_2 + \frac{K_2}{z}\right)\sum_{i=0}^{n-2} u_i - \frac{1}{2}\left(L_1 + \frac{K_1}{z}\right)\sum_{i=0}^{n-2} v_i, \\
w_{n,x} &= \bar{L}_2 \bar{u}_{n-1} - \bar{L}_1 w_{n-1} + \frac{1}{2}(\bar{L}_2 + z\bar{K}_2)\sum_{i=0}^{n-2} \bar{u}_i - \frac{1}{2}(\bar{L}_1 + z\bar{K}_1)\sum_{i=0}^{n-2} w_i, \\
w_{n,y} &= \bar{K}_2 \bar{u}_{n-1} - \bar{K}_1 w_{n-1} + \frac{1}{2}\left(\bar{K}_2 + \frac{\bar{L}_2}{z}\right)\sum_{i=0}^{n-2} \bar{u}_i - \frac{1}{2}\left(\bar{K}_1 + \frac{\bar{L}_1}{z}\right)\sum_{i=0}^{n-2} w_i,
\end{aligned} \tag{50}$$

with $\bar{u}_i$ *being given by formulas* (49).

By construction, equations (50) are compatible and yield a triple hierarchy of conservation laws of the CAE.

It follows that hierarchies u_i, v_i, w_i are independent, as we have shown in the last section of [26].

Proposition 6.4.4. *There is no possible functional dependence among the potentials* u_i, v_i, w_i.

7 Iteration of the superposition principle for the CAE

In this section, results from [25] are summarized. The most important result is a formula solving the recurrences from Prop. 2.3.1.

Proposition 7.0.5. *Let x_1, y_1, g_1 be the associated potentials corresponding to the pair $\omega^{[0]}, \omega^{[1]}$ of sine-Gordon solutions. Let $S^{[j]}$ be 4×4 matrices with entries defined by formulas*

$$
\begin{aligned}
S^{[j]}_{11} &= \frac{\lambda_{j+1}\lambda_1}{\lambda_{j+1}^2 - \lambda_1^2},\\
S^{[j]}_{13} &= -\frac{\lambda_{j+1}^2\lambda_1^2}{\lambda_{j+1}^2 - \lambda_1^2} \times \frac{2\sin\dfrac{\bar{\omega}^{[j]} - \omega^{[j]}}{2}}{\lambda_{j+1}^2 + \lambda_1^2 - 2\lambda_{j+1}\lambda_1\cos\dfrac{\bar{\omega}^{[j]} - \omega^{[j]}}{2}},\\
S^{[j]}_{22} &= \frac{\lambda_{j+1}^2 - \lambda_1^2}{\lambda_{j+1}\lambda_1}, \quad S^{[j]}_{24} = -2\sin\frac{\bar{\omega}^{[j]} - \omega^{[j]}}{2},\\
S^{[j]}_{33} &= \frac{1}{S^{[j]}_{44}} = \frac{-\lambda_{j+1}\lambda_1}{\lambda_{j+1}^2 + \lambda_1^2 - 2\lambda_{j+1}\lambda_1\cos\dfrac{\bar{\omega}^{[j]} - \omega^{[j]}}{2}}
\end{aligned}
\tag{51}
$$

all the other entries being zero. Let

$$
\begin{pmatrix} x^{[n]} \\ y^{[n]} \\ g^{[n]} \\ 1/g^{[n]} \end{pmatrix} = \left(\prod_{i=1}^{n-1} S^{[i]}\right) \begin{pmatrix} x_1 \\ y_1 \\ g_1 \\ 1/g_1 \end{pmatrix}. \tag{52}
$$

Then $x^{[n]}, y^{[n]}, g^{[n]}$ are the associated potentials corresponding to the pair $\bar{\omega}^{[n-1]}, \omega^{[n]}$. Moreover, if $z^{[n]} = 1/{g^{[n]}}^2$, then $z^{[n]}(x^{[n]}, y^{[n]})$ is a solution of the constant astigmatism equation (5).

7.1 Multisoliton solutions

Let $\omega^{[0]} = 0$. Let us define

$$a_i := \mathrm{e}^{\lambda_i \xi + \eta/\lambda_i + c_i},$$

c_i being constants. Solving the system (10), we reveal one-soliton solutions of the sine-Gordon equation

$$\omega^{[1]} = 4\arctan a_1, \qquad \bar{\omega}^{[1]} = 4\arctan a_2 \tag{53}$$

and, applying the superposition principle (11) to the triple $\omega^{[0]}, \omega^{[1]}, \bar{\omega}^{[1]}$, we easily obtain the two-soliton solutions

$$\begin{aligned} \omega^{[2]} &= 4 \arctan \frac{(\lambda_1 + \lambda_2)(a_1 - a_2)}{(\lambda_1 - \lambda_2)(1 + a_1 a_2)}, \\ \bar{\omega}^{[2]} &= 4 \arctan \frac{(\lambda_2 + \lambda_3)(a_2 - a_3)}{(\lambda_2 - \lambda_3)(1 + a_2 a_3)}. \end{aligned} \tag{54}$$

An exact analytic n-soliton solution, in our notation $\omega^{[n]}$, of the sine-Gordon equation has been obtained by several authors [1, 12, 13, 14, 15, 21], see also [3, 49]. The formula best suited for this paper can be found e.g. in [15] and is of the form

$$\omega^{[n]} = \arccos \varphi^{[n]}, \tag{55}$$

where

$$\varphi^{[n]} = 1 - 2 \frac{\partial^2}{\partial \xi \, \partial \eta} \ln \det M \tag{56}$$

M being the $n \times n$ matrix with entries

$$M_{ij} = \frac{1}{\lambda_i + \lambda_j} \left(\sqrt{a_i a_j} + \frac{1}{\sqrt{a_i a_j}} \right).$$

Note also that $\bar{\omega}^{[n]}$ arises from $\omega^{[n]}$ by increasing all lambdas' indices by one, namely

$$\bar{\omega}^{[n]} = \arccos \bar{\varphi}^{[n]}, \tag{57}$$

where

$$\bar{\varphi}^{[n]} = 1 - 2 \frac{\partial^2}{\partial \xi \, \partial \eta} \ln \det \overline{M} \tag{58}$$

and

$$\overline{M}_{ij} = \frac{1}{\lambda_{i+1} + \lambda_{j+1}} \left(\sqrt{a_{i+1} a_{j+1}} + \frac{1}{\sqrt{a_{i+1} a_{j+1}}} \right).$$

Definition 7.1.1. By a *j-soliton solution of the constant astigmatism equation* we shall mean a triple $(x^{[j]}, y^{[j]}, g^{[j]})$ formed by associated potentials corresponding to the j-soliton solution $\omega^{[j]}$ and the $(j-1)$-soliton solution $\bar\omega^{[j-1]}$ (see diagram (18)) of the sine-Gordon equation.

Remark 7.1.1. To obtain a solution of the CAE explicitly, one would have to express $z^{[j]} = 1/{g^{[j]}}^2$ in terms of $x^{[j]}$ and $y^{[j]}$. However, this is almost never possible in terms of elementary functions.

A one-soliton solution of the CAE is easy to construct. Following (15), $x^{[1]} = x_1$ and $g^{[1]} = g_1$ can be obtained by differentiation, namely

$$g_1 = \frac{\mathrm{d}\omega^{[1]}}{\mathrm{d}c_1} = \frac{4a_1}{a_1^2+1}, \qquad x_1 = -2\frac{\mathrm{d}\ln g_1}{\mathrm{d}c_1} = 2\frac{a_1^2-1}{a_1^2+1}. \tag{59}$$

For $y^{[1]} = y_1$ we have the system

$$\begin{aligned} y^{[1]}_\xi &= \frac{\lambda_1 \sin(\omega^{[1]} + \bar\omega^{[0]})}{g_1} = \frac{\lambda_1}{2}, \\ y^{[1]}_\eta &= -\frac{\sin(\omega^{[1]} - \bar\omega^{[0]})}{\lambda_1 g_1} = -\frac{1}{2\lambda_1} \end{aligned}$$

with the general solution

$$y_1 = \frac{\lambda_1}{2}\xi - \frac{\eta}{2\lambda_1} + k_1, \tag{60}$$

k_1 being an arbitrary constant. Setting $z_1 = 1/g_1^2$, eliminating ξ, η and dropping the lower indices, one reveals the von Lilienthal solution

$$z = \frac{1}{4-x^2}, \tag{61}$$

see Fig. 15.

Proposition 7.1.1. *Let us denote*

$$A^{[j]} = 2\bar\varphi^{[j]}\varphi^{[j]} \quad \text{and} \quad B^{[j]} = 2\sqrt{({\bar\varphi^{[j]}}^2 - 1)({\varphi^{[j]}}^2 - 1)}\,,$$

where $\varphi^{[j]}$ *and* $\bar{\varphi}^{[j]}$ *are defined by* (56) *and* (58) *respectively. Then the n-soliton solution of the CAE is given by the formula*

$$\begin{pmatrix} x^{[n]} \\ y^{[n]} \\ g^{[n]} \\ 1/g^{[n]} \end{pmatrix} = \left(\prod_{i=1}^{n-1} S^{[i]} \right) \begin{pmatrix} x_1 \\ y_1 \\ g_1 \\ 1/g_1 \end{pmatrix}, \tag{62}$$

where the only nonzero entries of matrices $S^{[j]}$ *are given by*

$$\begin{aligned} S_{11}^{[j]} &= \frac{\lambda_{j+1}\lambda_1}{\lambda_{j+1}^2 - \lambda_1^2}, \\ S_{13}^{[j]} &= \frac{\lambda_{j+1}^2\lambda_1^2}{\lambda_1^2 - \lambda_{j+1}^2} \cdot \frac{\sqrt{2 - A^{[j]} - B^{[j]}}}{\lambda_1^2 + \lambda_{j+1}^2 - \lambda_{j+1}\lambda_1\sqrt{2 + A^{[j]} + B^{[j]}}} \\ S_{22}^{[j]} &= \frac{\lambda_{j+1}^2 - \lambda_1^2}{\lambda_{j+1}\lambda_1}, \qquad S_{24}^{[j]} = -\sqrt{2 - A^{[j]} - B^{[j]}}, \\ S_{33}^{[j]} &= \frac{1}{S_{44}^{[j]}} = \frac{-\lambda_{j+1}\lambda_1}{\lambda_1^2 + \lambda_{j+1}^2 - \lambda_{j+1}\lambda_1\sqrt{2 + A^{[j]} + B^{[j]}}}. \end{aligned} \tag{63}$$

Formulas (63) follow from plugging (55) and (57) into (51) and employing trigonometric identities.

7.2 Multisoliton surfaces of constant astigmatism

Let us adapt the notation from Subsect. 2.3, i.e. let us define (cf. (19))

$$\mathbf{r}^{[k]} = \mathbf{r}^{(\lambda_1\lambda_2\ldots\lambda_k)}, \qquad \bar{\mathbf{r}}^{[k]} = \mathbf{r}^{(\lambda_2\lambda_3\ldots\lambda_{k+1})}.$$

Then we have the recurrence relation (cf. (12))

$$\begin{aligned} &\mathbf{r}^{[j+1]} = \\ &\mathbf{r}^{[j]} + \frac{2\lambda_{j+1}\csc\omega^{[j]}}{1 + \lambda_{j+1}^2}\left[\sin\left(\frac{\omega^{[j]} - \omega^{[j+1]}}{2}\right)\mathbf{r}_\xi^{[j]} + \sin\left(\frac{\omega^{[j]} + \omega^{[j+1]}}{2}\right)\mathbf{r}_\eta^{[j]}\right] \end{aligned} \tag{64}$$

with the initial condition $\mathbf{r}^{[0]} = \bar{\mathbf{r}}^{[0]} = \mathbf{r}_0$. Surfaces $\bar{\mathbf{r}}^{[i]}$ are obtained from $\mathbf{r}^{[i]}$ simply by increasing all lambdas' indices by one and replacing $\omega^{[i]}$ with $\bar{\omega}^{[i]}$.

The iteration process is shown in the diagram below, cf. (18).

$$\begin{array}{ccccccccccc}
\mathbf{r}^{[0]} & \xrightarrow{\lambda_2} & \bar{\mathbf{r}}^{[1]} & \xrightarrow{\lambda_3} & \bar{\mathbf{r}}^{[2]} & \xrightarrow{\lambda_4} & \bar{\mathbf{r}}^{[3]} & \xrightarrow{\lambda_5} & \bar{\mathbf{r}}^{[4]} & \xrightarrow{\lambda_6} & \cdots \\
\lambda_1 \downarrow & & \lambda_1 \downarrow & & \lambda_1 \downarrow & & \lambda_1 \downarrow & & \lambda_1 \downarrow & & \\
\mathbf{r}^{[1]} & \xrightarrow{\lambda_2} & \mathbf{r}^{[2]} & \xrightarrow{\lambda_3} & \mathbf{r}^{[3]} & \xrightarrow{\lambda_4} & \mathbf{r}^{[4]} & \xrightarrow{\lambda_5} & \mathbf{r}^{[5]} & \xrightarrow{\lambda_6} & \cdots
\end{array} \tag{65}$$

Recall that substituting $\lambda = 1$ into (12) one gets a complementary pseudospherical surface (13). Obviously, the surfaces $\mathbf{r}^{[j]}$ and $\bar{\mathbf{r}}^{[j-1]}$ become complementary when substituting $\lambda_1 = 1$ into $\mathbf{r}^{[j]}$.

The common involute, $\tilde{\mathbf{r}}^{[j]}$, of a pair of complementary pseudospherical surfaces, $\mathbf{r}^{[j]}|_{\lambda_1=1}$ and $\bar{\mathbf{r}}^{[j-1]}$, is of constant astigmatism and is given by (17). In our notation, the equation turns out to be

$$\tilde{\mathbf{r}}^{[j]} = \bar{\mathbf{r}}^{[j-1]} - \tilde{\mathbf{n}}^{[j]} \ln g^{[j]}|_{\lambda_1=1},$$

where $g^{[j]}$ is determined by (52) and $\tilde{\mathbf{n}}^{[j]}$, a unit normal of the constant astigmatism surface, is simply

$$\tilde{\mathbf{n}}^{[j]} = \mathbf{r}^{[j]}|_{\lambda_1=1} - \bar{\mathbf{r}}^{[j-1]}.$$

Definition 7.2.1. If the surfaces $\mathbf{r}^{[j]}|_{\lambda_1=1}$ and $\bar{\mathbf{r}}^{[j-1]}$ are j-soliton and $(j-1)$-soliton pseudospherical surfaces respectively, then the corresponding common involute, $\tilde{\mathbf{r}}^{[j]}$, will be called a *j-soliton surface of constant astigmatism.*

Let us also remark that $\tilde{\mathbf{n}}^{[j]}(\xi, \eta)$ parameterises a unit sphere by slip lines (see Sect. 3).

7.3 Examples of multisoliton solutions

Following previous part of this section, it is a matter of routine to generate examples of multisoliton solutions of the CAE as well as corresponding constant astigmatism surfaces and slip line fields. Unfortunately, construction of orthogonal equiareal patterns quickly leaves the realm of elementary functions.

Throughout this section we provide pictures of the surfaces, solutions and slip line fields; all formulas are to be found in [25]. We use the notation from diagrams (18) and (65).

The n-soliton pseudospherical surfaces are easy to compute, see Fig. 14.

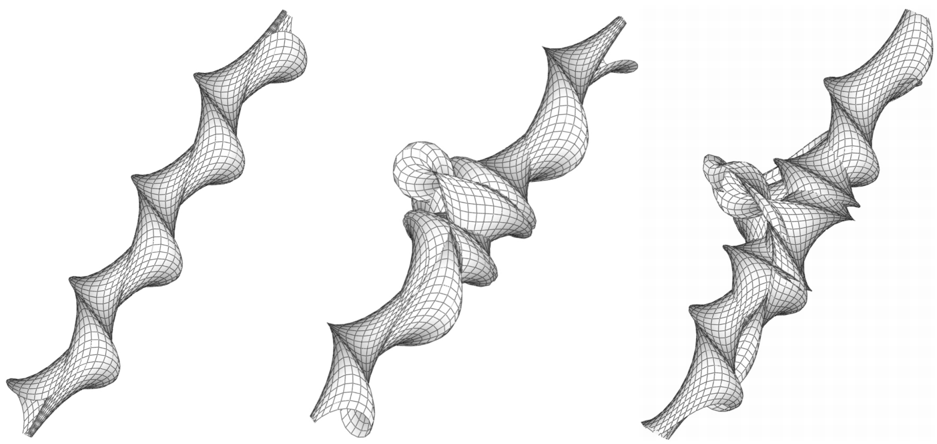

Figure 14: From the left: One-, two- and three-soliton pseudospherical surfaces, $\bar{\mathbf{r}}^{[1]}, \mathbf{r}^{[2]}, \mathbf{r}^{[3]}$ respectively, $\lambda_1 = 1$, $\lambda_2 = 1.5$, $\lambda_3 = 1.8$. The leftmost is the surface of Dini.

7.3.1 One-soliton solutions

One-soliton solution $z^{[1]}(x^{[1]}, y^{[1]})$, corresponding to the pair $\omega^{[0]}$ and $\omega^{[1]}$, has been already constructed, see (61) and Fig. 15. Corresponding surfaces $\tilde{\mathbf{r}}^{[1]}$ of constant astigmatism coincide with the von Lilienthal class, see Fig. 2. Evolutes of the surface $\tilde{\mathbf{r}}^{[1]}$ are the pseudosphere $\mathbf{r}^{[1]}|_{\lambda_1=1}$ and the z-axis $\mathbf{r}^{[0]} = (0, 0, \xi+\eta)$. The slip line field $\tilde{\mathbf{n}}^{[1]}$ can be seen in Fig. 4 as well as corresponding orthogonal equiareal pattern, which is the Archimedean projection.

7.3.2 Two-soliton solutions

A plot of two-soliton solution $z^{[2]}(x^{[2]}, y^{[2]})$, corresponding to the pair $\bar{\omega}^{[1]}$ and $\omega^{[2]}$, can be seen in Fig. 16.

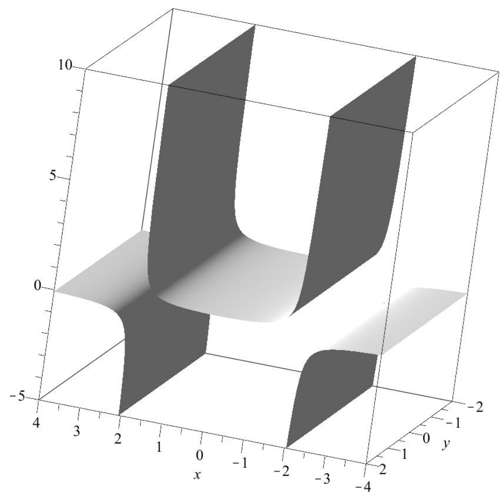

Figure 15: Solution $z = 1/(4 - x^2)$ of the CAE. One can clearly see that the solution is geometrically admissible when $-2 < x < 2$.

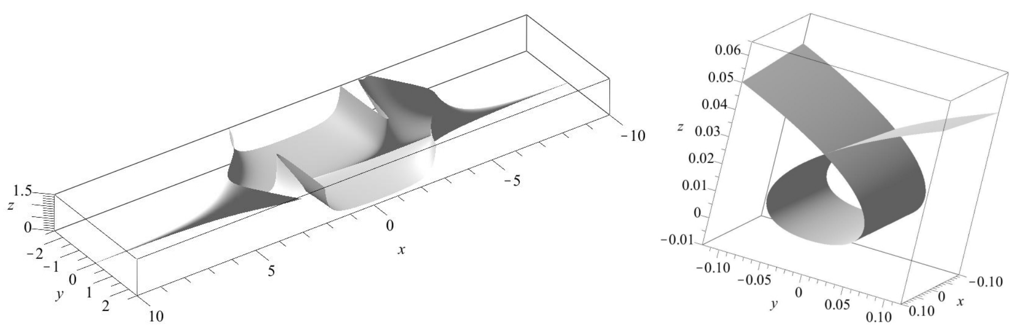

Figure 16: Two soliton solution of the CAE, $\lambda_1 = 1.2$, $\lambda_2 = 1.5$. Right part of the figure shows the behavior around the origin.

Corresponding surfaces $\tilde{\mathbf{r}}^{[2]}(\xi, \eta)$ of constant astigmatism are plotted in Fig. 17. Evolutes of the surface $\tilde{\mathbf{r}}^{[2]}$ are $\mathbf{r}^{[2]}|_{\lambda_1=1}$ and the Dini's surface $\bar{\mathbf{r}}^{[1]}$. For the slip line field $\tilde{\mathbf{n}}^{[2]}(\xi, \eta)$ see Fig. 18. To obtain an associated orthogonal equiareal pattern one needs to invert the transformation $(x^{[2]}, y^{[2]}) \leftrightarrow (\xi, \eta)$, which is not possible in terms of elementary functions.

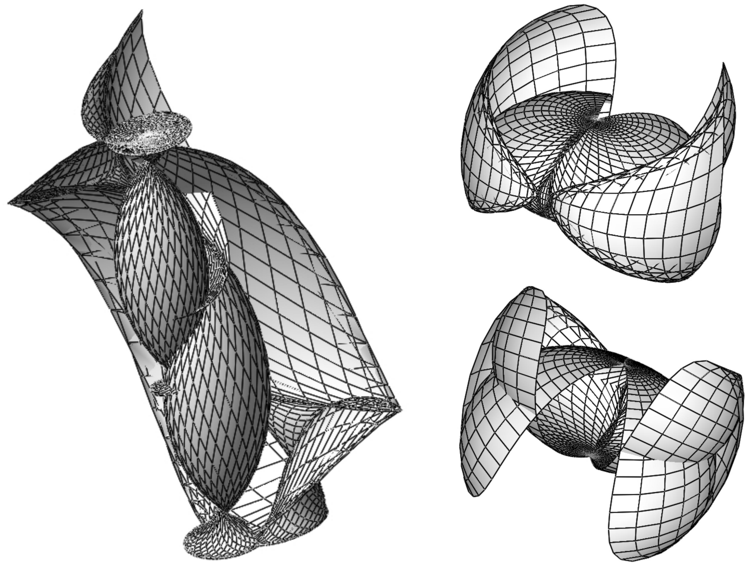

Figure 17: Two soliton surfaces $\tilde{\mathbf{r}}^{[2]}(\xi, \eta)$ of constant astigmatism, $\lambda_2 = 1.5$ (left) and its limit for $\lambda_2 \to 1$ (right). The second surface is displayed from two views under the parameterisation by $(\Xi, \Theta) = (\xi + \eta, \xi - \eta)$.

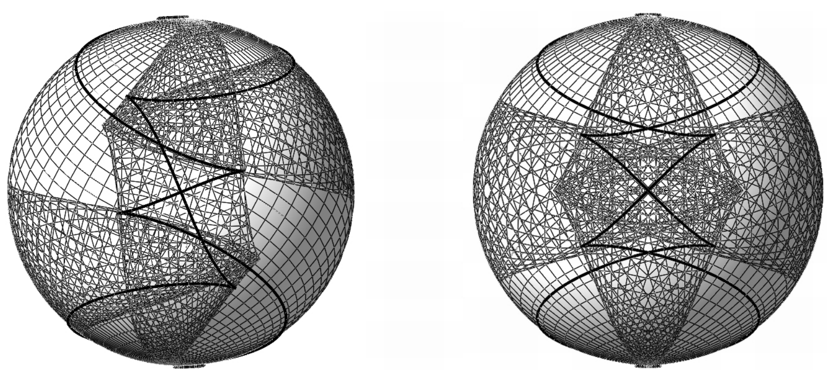

Figure 18: Slip line field $\tilde{\mathbf{n}}^{[2]}(\xi, \eta)$, $\lambda_2 = 1.5$, $c_i = 0$ (left) and its limit for $\lambda_2 \to 1$ (right) with coordinate lines $\xi = 0$ and $\eta = 0$ highlighted (thick black curves).

7.3.3 Three-soliton solutions

A plot of three-soliton solution $z^{[3]}(x^{[3]}, y^{[3]})$, corresponding to the pair $\bar{\omega}^{[2]}$ and $\omega^{[3]}$, is displayed in Fig. 19, a multivaluedness of the function z being clearly identified. In the right side of the figure (values of z near the point $(0,0,0)$) one can observe that at least eight values of z may correspond to one particular choice of x and y.

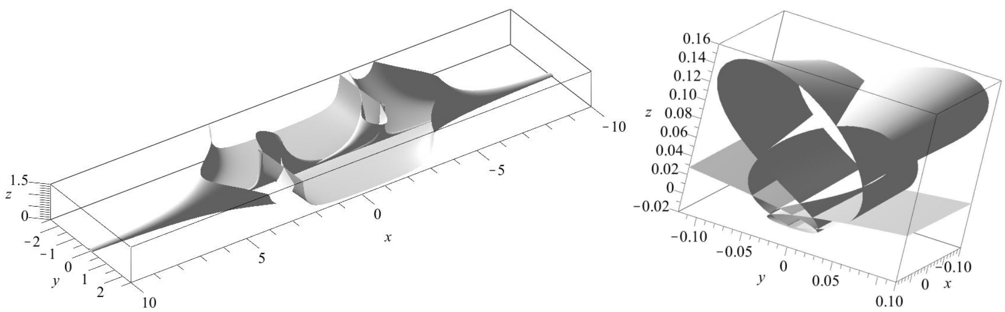

Figure 19: Three soliton solution of the CAE, $\lambda_1 = 1.2$, $\lambda_2 = 1.5$, $\lambda_3 = 1.8$. Right part of the figure shows the behavior around the origin.

Corresponding surfaces $\tilde{\mathbf{r}}^{[3]}(\xi, \eta)$ of constant astigmatism are plotted in Fig. 20. Evolutes of the surface $\tilde{\mathbf{r}}^{[3]}$ are $\mathbf{r}^{[3]}|_{\lambda_1=1}$ and $\bar{\mathbf{r}}^{[2]}$. For the slip line field $\tilde{\mathbf{n}}^{[3]}(\xi, \eta)$ see Fig. 21. It does not come as a surprise that obtaining an associated orthogonal equiareal pattern requires inverting of the transformation $(x^{[3]}, y^{[3]}) \leftrightarrow (\xi, \eta)$, which is not possible in terms of elementary functions.

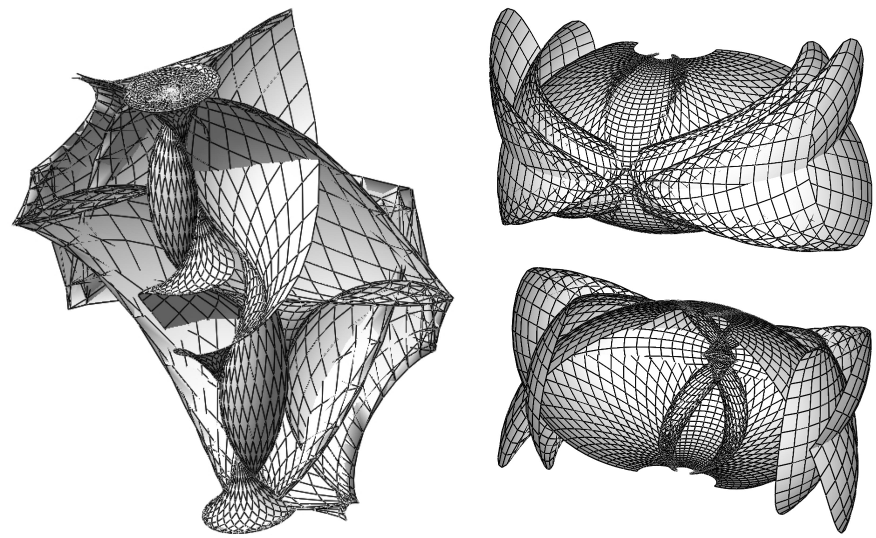

Figure 20: Three soliton surfaces $\tilde{\mathbf{r}}^{[3]}(\xi, \eta)$ of constant astigmatism, $\lambda_2 = 1.5$, $\lambda_3 = 1.8$ (left) and its limit for $(\lambda_2, \lambda_3) \to (1, 1)$ (right). The second surface is displayed from two views under the parameterisation by $(\Xi, \Theta) = (\xi{+}\eta, \xi{-}\eta)$.

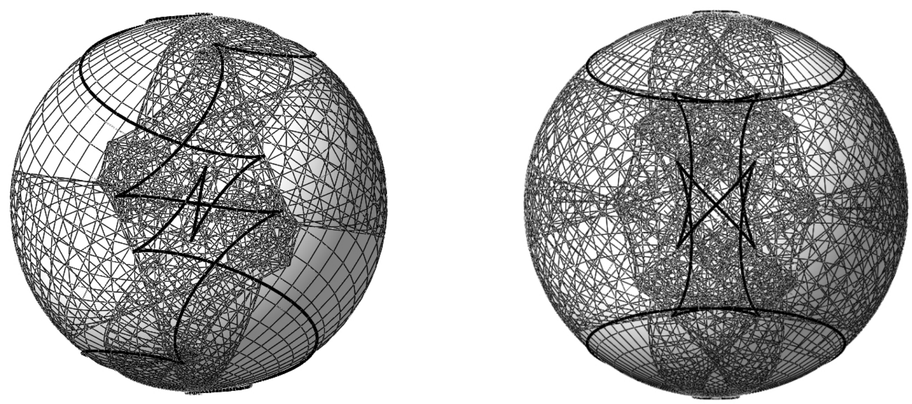

Figure 21: Slip line field $\tilde{\mathbf{n}}^{[3]}$, $\lambda_2 = 1.5$, $\lambda_3 = 1.8$, (left) and its limit for $(\lambda_2, \lambda_3) \to (1, 1)$ (right) with coordinate lines $\xi = 0$ and $\eta = 0$ highlighted (thick black curves).

8 More exact solutions of the CAE

The last section of the thesis summarizes the work [27]. In the paper, we construct another seed solution of the CAE which is ready to be transformed to infinite number of new solutions by nonlinear superposition formula (52). Since the zero sine-Gordon solution was succesfully planted in previous section, we deal with a *nonzero* sine-Gordon seed and its Bäcklund transformation. Techniques for obtaining such pairs can be found e.g. in [28] or [20]; the simplest initial sine-Gordon solution being the so called “travelling wave”. As we know from Sect. 4, Prop. 4.4.1, the corresponding solutions of the CAE are the Lipschitz solutions.

In other words, in this section, we are going to reproduce Lipschitz solutions to obtain an infinite set of new solutions from it. However, the explicit form of the general Lipschitz solution as introduced in Sect. 4, Thm. 4.2.1, is not suitable for our approach; we seek the seed solution parameterised by coordinates ξ, η in order to be prepared for the formula (52).

8.1 Construction of a seed solution

According to Prop. 4.4.1, solutions of the sine-Gordon equation corresponding to Lipchitz's solutions of the CAE satisfy

$$\omega_\xi = k\omega_\eta, \tag{66}$$

where k is a nonzero constant. Thus, they are of the form $\omega(k\xi + \eta + C)$, where C is a constant. Let us perform a transformation to new coordinates $\alpha = k\xi + \eta$ and $\beta = k\xi - \eta$ in which the sine-Gordon equation turns out to be

$$\omega_{\alpha\alpha} - \omega_{\beta\beta} = \frac{1}{k} \sin \omega.$$

The condition (66) reduces to

$$\omega_\beta = 0$$

and, therefore, the seed sine-Gordon solutions we are working with depend solely on α and they satisfy the ODE

$$k\omega_{\alpha\alpha} = \sin \omega. \tag{67}$$

Multiplying both sides of (67) by ω_α and integrating, one can reduce the order of the equation which becomes

$$k\omega_\alpha^2 = -2\cos\omega + 2l,$$

l being a constant. Solving for ω_α we obtain

$$\omega_\alpha = \pm\sqrt{\frac{2l - 2\cos\omega}{k}}. \tag{68}$$

Let ω be a solution of (67). According to [28], its Bäcklund transformation $\omega^{(\lambda)}$ can be written as

$$\omega^{(\lambda)} = 4\arctan\Big(\frac{f}{ak^2} + \frac{c}{ak}\tanh[c(\beta + b(\alpha) + K)]\Big) - \omega, \tag{69}$$

where

$$\begin{aligned} a &= \frac{\sin\omega}{4k\lambda} - \frac{\omega_\alpha}{4k}, \qquad f = \frac{\lambda}{4} - \frac{k\cos\omega}{4\lambda}, \\ c &= \frac{\sqrt{\lambda^4 - 2kl\lambda^2 + k^2}}{4k\lambda} = \text{const} \end{aligned} \tag{70}$$

and $b(\alpha)$ satisfies

$$b_\alpha = \frac{\lambda\omega_\alpha + \sin\omega}{\lambda\omega_\alpha - \sin\omega}. \tag{71}$$

Proposition 8.1.1. *Let ω be a solution of* (67) *and let $\omega^{(\lambda)}$, given by* (69), *be its Bäcklund transformation with parameter λ. Let a, f, c be defined by* (70) *and let b satisfy* (71). *Then the associated potentials $x^{(\lambda)}, y^{(\lambda)}, g^{(\lambda)}$ corresponding to the pair $\omega, \omega^{(\lambda)}$ are given by formulas*

$$\begin{aligned} x^{(\lambda)} &= \frac{8c^2kf\cosh 2B + 4c(f^2 + k^4a^2 + c^2k^2)\sinh 2B}{(f^2 + k^4a^2 + c^2k^2)\cosh 2B + 2ckf\sinh 2B + f^2 + k^4a^2 - c^2k^2}, \\ y^{(\lambda)} &= \Big(\frac{f\sin\omega}{16\lambda c^2k^2a} - \frac{2f - \lambda}{8c^2k}\Big)\cosh 2B \\ &- \Big(\frac{(k^4a^2 - c^2k^2 - f^2)\sin\omega}{32\lambda c^3k^3a} + \frac{f(2f - \lambda)}{8c^3k^2}\Big)\sinh 2B \\ &+ \frac{1}{\lambda^4 - 2kl\lambda^2 + k^2}\bigg(\frac{\lambda^4 - k^2}{2}\beta + \frac{\lambda^4 + k^2}{2}\alpha - k\lambda^2\int\cos\omega\,\mathrm{d}\alpha\bigg), \\ g^{(\lambda)} &= \frac{4c^2k^3a(1 - \tanh^2 B)}{k^4a^2 + f^2 + 2ckf\tanh B + c^2k^2\tanh^2 B}, \end{aligned} \tag{72}$$

where $B = c(\beta + b + K)$ *and* l *is a constant. Moreover, if* $z^{(\lambda)} = 1/{g^{(\lambda)}}^2$*, then* $z^{(\lambda)}(x^{(\lambda)}, y^{(\lambda)})$ *is a solution of the constant astigmatism equation* (5)*.*

Remark 8.1.1. According to [16], we have the following results of integration of (68),

- for $l/k > 1/k$ (case A)
$$\omega_0 = 2 \arccos\left[\operatorname{sn}\left(\frac{-\alpha p}{\sqrt{k}}; \frac{1}{p}\right)\right], \tag{73}$$
- for $|l/k| < 1/k$ (case B)
$$\omega_0 = 2 \arcsin\left[\operatorname{dn}\left(\frac{\alpha}{\sqrt{k}}; p\right)\right], \tag{74}$$
- for $l = 1$ (case C)
$$\omega_0 = 4 \arctan\left(\exp \frac{\alpha}{\sqrt{k}}\right), \tag{75}$$

where we have denoted
$$p = \sqrt{\frac{1+l}{2}}. \tag{76}$$

Note that case C coincides with one-soliton solution of the sine-Gordon equation, cf. (53). Hence, the case when $l = 1$ is taken out of consideration in the sequel.

Remark 8.1.2. A closer look shows that the solution (72) is periodic in the y-direction. Indeed, the shifts $\alpha \longmapsto \alpha + 4\sqrt{k}\,\mathrm{K}(p)$ (in case A) and $\alpha \longmapsto \alpha + 2\sqrt{k}\,\mathrm{K}(p)$ (in case B) leave $x^{(\lambda)}$ and $g^{(\lambda)}$ unchanged, while the $y^{(\lambda)}$ is translated by

$$P_{\mathrm{A}} = \mathfrak{Re}\left(\frac{2\sqrt{k}\,[(k+\lambda^2)^2 - 4k\lambda^2p^2]\,\mathrm{K}(p)}{(k+\lambda^2)^2 - 4k^2\lambda^2} + \frac{8k^{\frac{3}{2}}\lambda^2 p\,\mathrm{E}\Big[\operatorname{sn}\Big(p\,\mathrm{K}(p), \frac{1}{p}\Big), \frac{1}{p}\Big]}{(k+\lambda^2)^2 - 4k^2\lambda^2}\right)$$

in case A and by

$$P_{\rm B} = \frac{2\sqrt{k}\,(k-\lambda^2)^2}{(k+\lambda^2)^2 - 4k^2\lambda^2}\,{\rm K}(p) + \frac{8k^{\frac{3}{2}}\lambda^2}{(k+\lambda^2)^2 - 4k^2\lambda^2}\,{\rm E}(p)$$

in case B. Here K and E denote complete elliptic integrals of the first and the second kind respectively. Finally, a detailed look at the formula (52) reveals that the n-th solution, arising from the periodic seed (72), is also periodic with period $P_{\rm A} \times (\prod_{i=1}^{n-1} S_{22}^{[i]})$ in case A and $P_{\rm B} \times (\prod_{i=1}^{n-1} S_{22}^{[i]})$ in case B.

A graph of the solution $z(x,y) = z^{(\lambda)}(x^{(\lambda)}, y^{(\lambda)})$, where x, y and $z = 1/g^2$ are given by (72) under the parameterisation by ξ, η, can be easily plotted for both cases A and B, see Fig. 22. Periodicity in y-direction can be clearly identified.

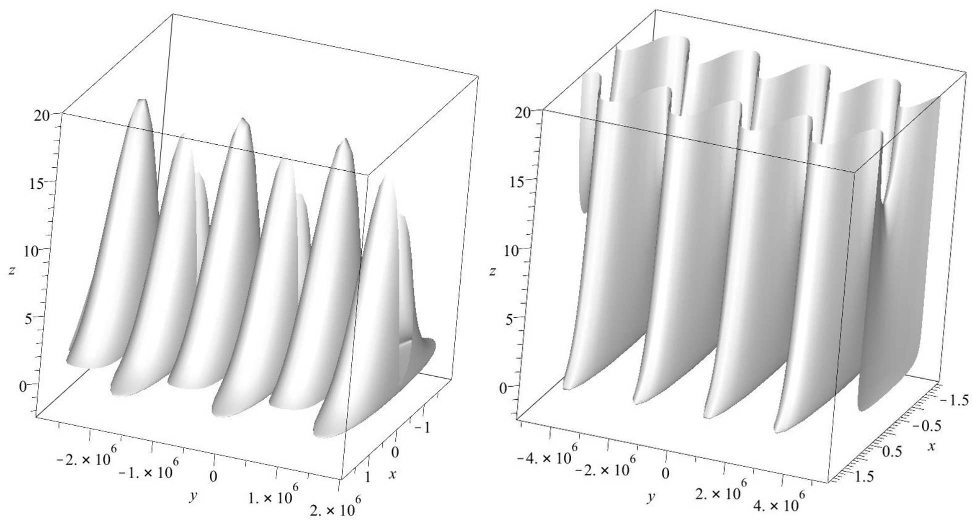

Figure 22: Solutions $z^{(\lambda)}(x^{(\lambda)}, y^{(\lambda)})$ of the CAE, $\lambda = 1.001$, $k = 1$, $K = 0$, $l = 3/2$ (case A, left), $l = 1/2$ (case B, right).

8.2 Surfaces of constant astigmatism

Pseudospherical surfaces corresponding to the solutions satisfying (66) were constructed by Zadadaev [54] and, according to [40], they coincide with surfaces studied in the 19th century by Minding [38], see also [10, 39]. In

Zadadaev's parameterisation by asymptotic coordinates the surfaces are given by formula

$$\mathbf{r}_0 = \frac{\sqrt{k}}{p(k+1)} \begin{pmatrix} 2\sin\dfrac{\omega_0}{2}\sin[p(\xi-\eta)] \\ 2\sin\dfrac{\omega_0}{2}\cos[p(\xi-\eta)] \\ \xi+\eta+\dfrac{1}{\sqrt{k}}\displaystyle\int\cos\omega_0\,\mathrm{d}\alpha \end{pmatrix}, \tag{77}$$

where $\omega_0 = \omega_0(\alpha) = \omega_0(k\xi + \eta)$ is one of the solutions (73)–(75) and the constants k, p have the same meaning as in the previous section, see (66) and (76). For pictures corresponding to all three cases, A, B and C, see Fig. 23, cf. [38, 54], [10, p. 192–193] or [39, p. 228].

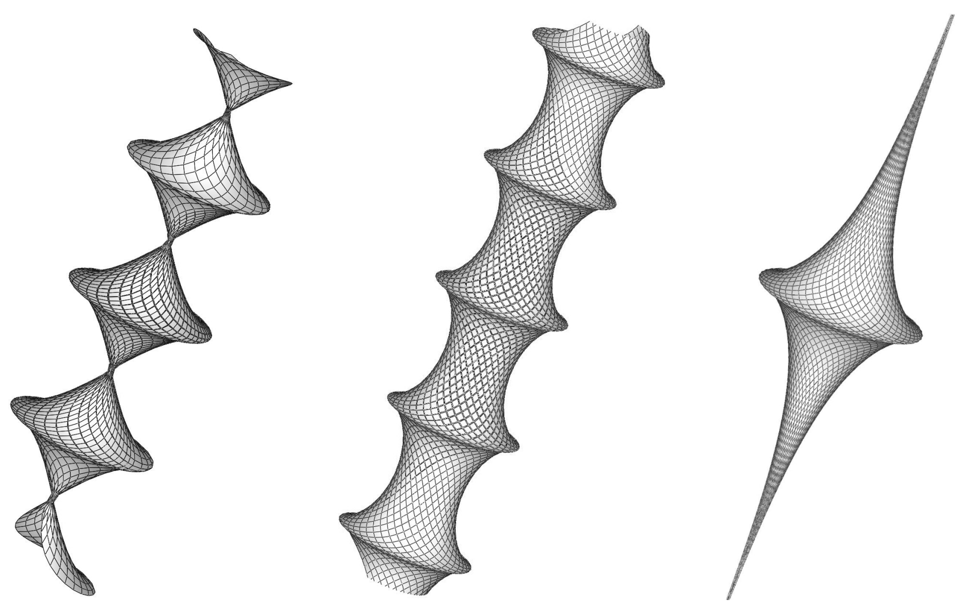

Figure 23: From the left: Minding's pseudospherical surfaces $\mathbf{r}_0$ (parameterised by ξ, η) corresponding to solutions (73), (74) and (75) respectively, $k = 1$, $l = 3/2$ (left), $l = 1/2$ (middle), $l = 1$ (right). The rightmost surface is the pseudosphere.

Using (12) we routinelly compute a Bäcklund transformation $\mathbf{r}^{(\lambda)}$ of the surface $\mathbf{r}_0$, see Fig. 24.

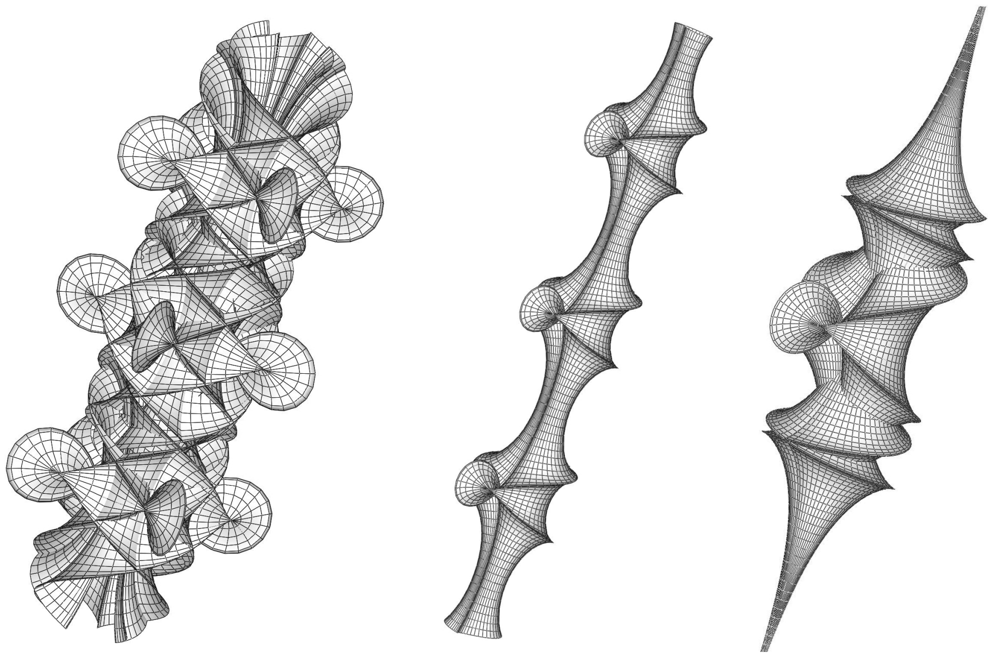

Figure 24: Transformed Minding's pseudospherical surfaces (parameterised by α, β) corresponding to cases A, B and C respectively, $k = 1, \lambda = 1, l = 3/2$ (left), $l = 1/2$ (middle), $l = 1$ (right). The righmost is the two-soliton Kuen's surface [31], see also [10, p. 470].

The corresponding family of constant astigmatism surfaces, the common involutes of complementary pseudospherical surfaces $\mathbf{r}_0$ and $\mathbf{r}^{(1)}$, can be easily computed using (17). Resulting surfaces are plotted in Figs. 25 and 26. The slip line field, $\tilde{\mathbf{n}}^{(1)}$, can be seen in Fig. 27.

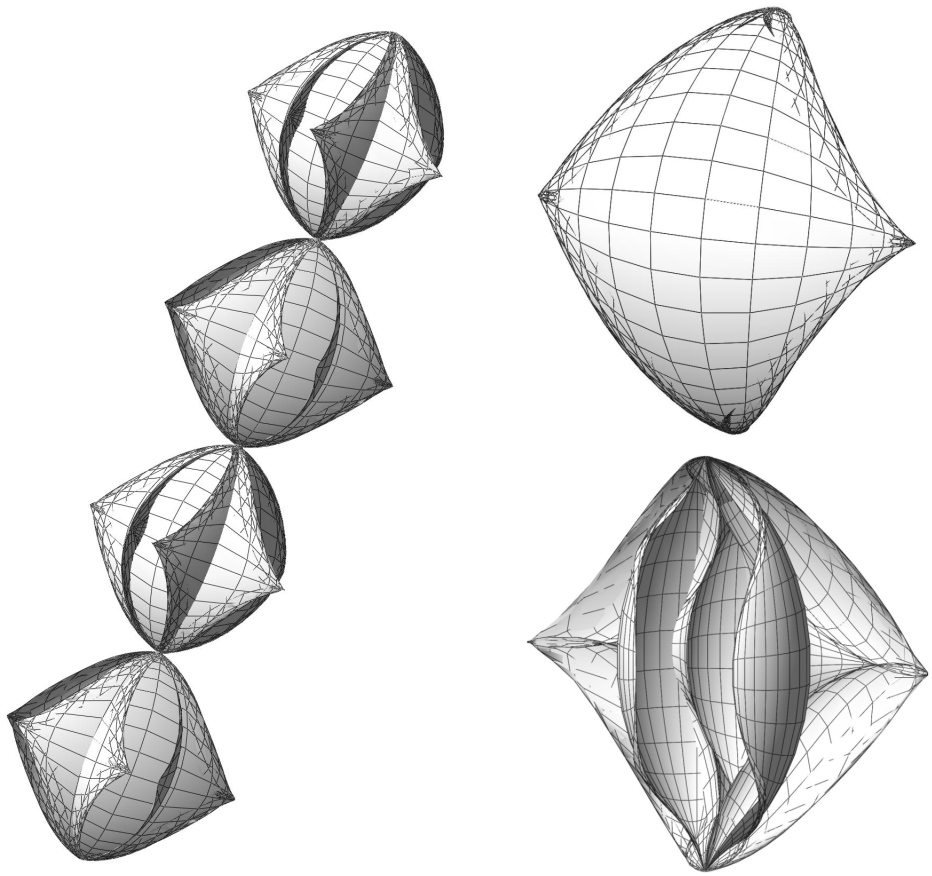

Figure 25: Constant astigmatism surface $\tilde{\mathbf{r}}^{(1)}$, parameterised by α, β, corresponding to case A. One of the pieces the surface is formed of is zoomed in the right. The piece is displayed from two mutually opposite directions.

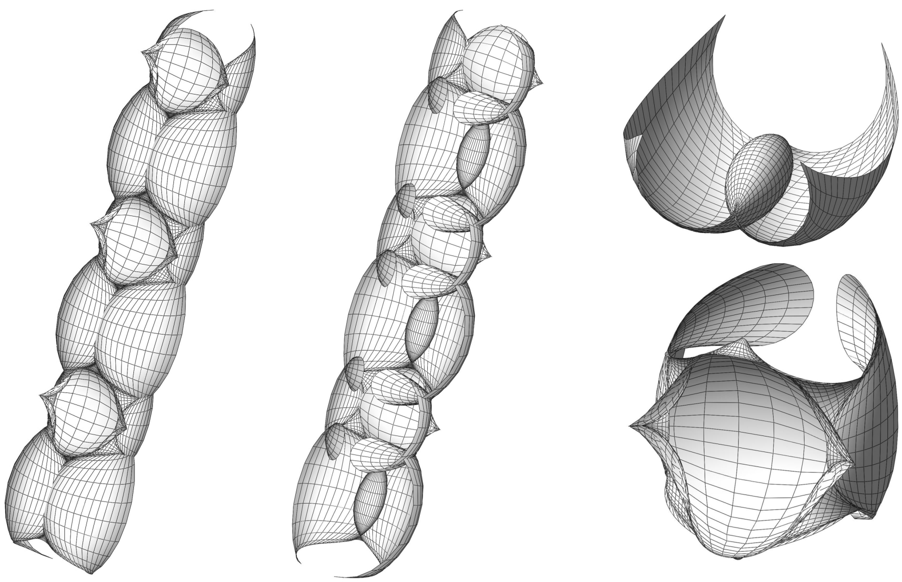

Figure 26: Constant astigmatism surface $\tilde{\mathbf{r}}^{(1)}$, parameterised by α, β, corresponding to case B. The first two pictures from the left show two views of the same surface from mutually opposite directions. The repeated pieces are zoomed in the right.

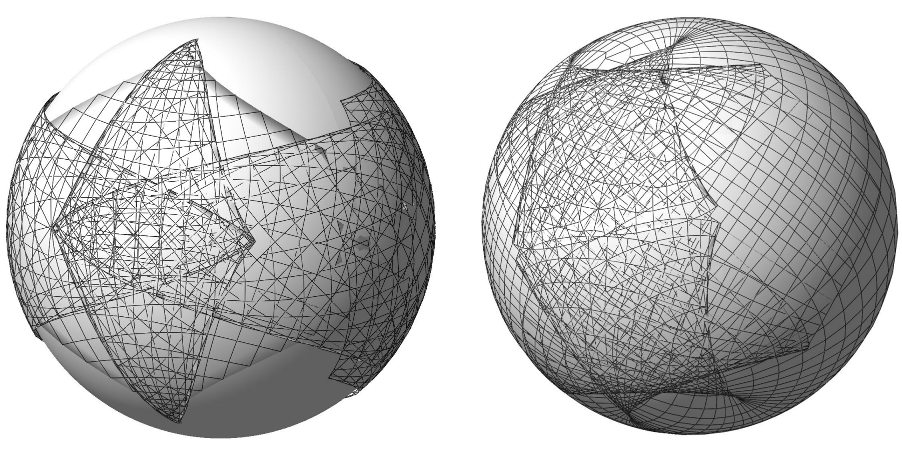

Figure 27: Slip line fields $\tilde{\mathbf{n}}^{(1)}(\xi, \eta)$ corresponding to case A (left) and case B (right).

Let us proceed to one more example. Using Proposition 7.0.5 we routinely construct solution $z^{(\lambda_1\lambda_2)}(x^{(\lambda_1\lambda_2)}, y^{(\lambda_1\lambda_2)})$ (see Fig. 28) from known solution $z^{(\lambda_1)}(x^{(\lambda_1)}, y^{(\lambda_1)})$. Twice transformed Minding's pseudospherical surfaces $\mathbf{r}^{(\lambda_1,\lambda_2)}$ can be also routinely computed, see Fig. 29. Corresponding constant astigmatism surfaces are plotted in Fig. 30.

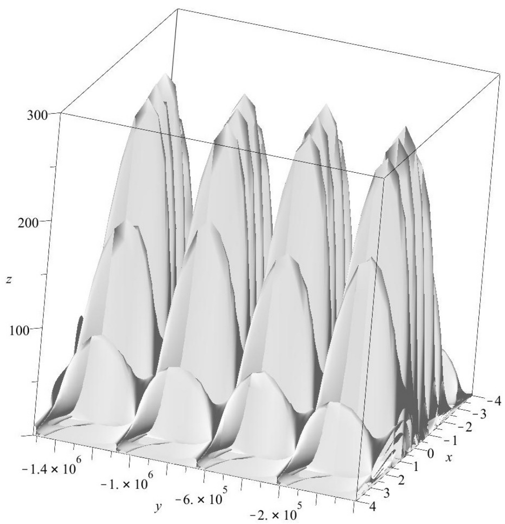

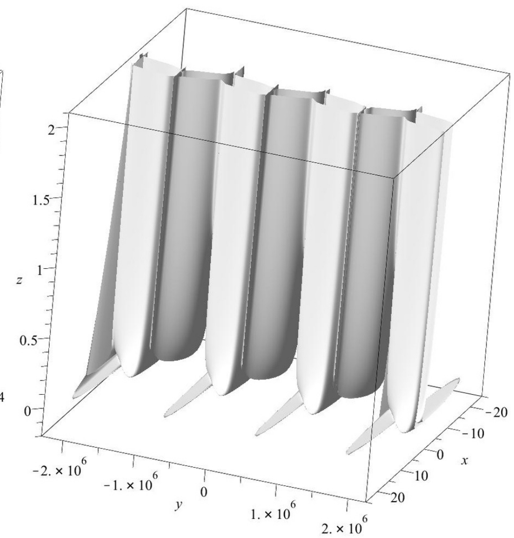

Figure 28: A rather complicated multivalued solutions $z^{(\lambda_1\lambda_2)}(x^{(\lambda_1\lambda_2)}, y^{(\lambda_1\lambda_2)})$ of the CAE that are periodic in the y-direction, $\lambda_1 = 1.001$, $\lambda_2 = 1.3$, $k = 1$, $K = 0$, $l = 3/2$ (case A, left), $l = 1/2$ (case B, right).

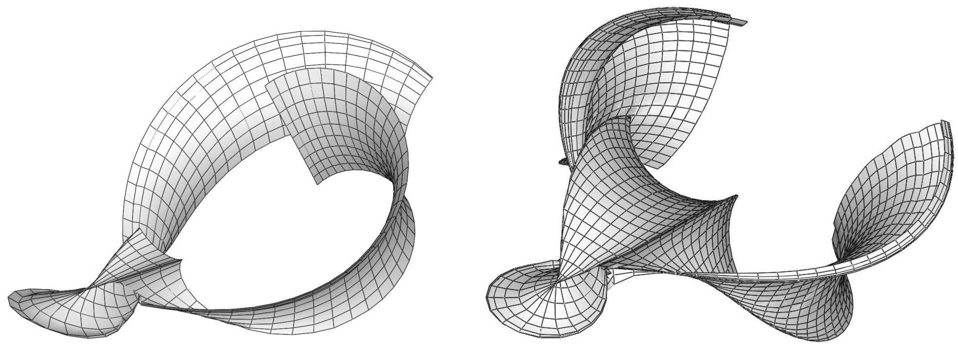

Figure 29: Pieces of pseudospherical surfaces $\mathbf{r}^{(\lambda_1\lambda_2)}$, parameterised by α, β, with $\lambda_1 = 1$, $\lambda_2 = 1.3$. Case A (left), case B (right).

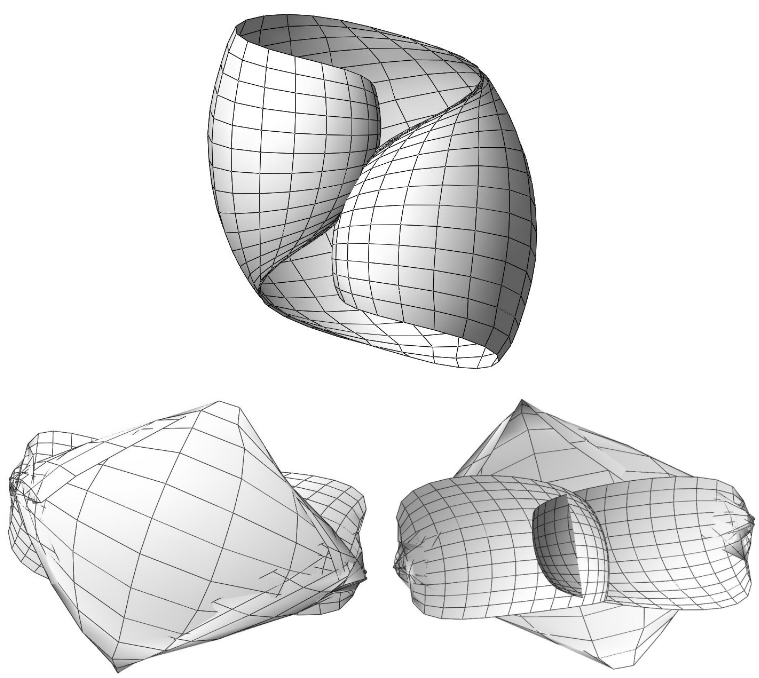

Figure 30: Two pieces of constant astigmatism surface, the common involute of $\mathbf{r}^{(\lambda_2)}$ and $\mathbf{r}^{(1\lambda_2)}$ with $\lambda_2 = 1.3$, case B. The second piece is displayed from two views. Surface is parameterised by α, β.

9 Presentations related to the thesis

- Mathematics in the modern world, August 2017, Novosibirsk, Russia.
  Talk: "More exact solutions of the constant astigmatism equation"

- Workshop on Integrable Systems, December 2016, Sydney, Australia.
  Talk: "On the constant astigmatism equation and surfaces of constant astigmatism"

- Nonlinear analysis and its applications, September 2016, Samarkand, Uzbekistan.
  Talk: "On the constant astigmatism equation and surfaces of constant astigmatism"

- Geometric methods in control theory and mathematical physics: differential equations, integrability, qualitative theory, September 2016, Ryazan, Russia.
  Talk: "On the constant astigmatism equation and surfaces of constant astigmatism"

- 7-th International Conference on Mathematical Analysis, Differential Equations & Their Applications MADEA-7, September 2015, Baku, Azerbaijan.
  Talk: "On multisoliton solutions of the constant astigmatism equation"

- International Congress of Mathematicians (ICM), August 2014, Coex, Seoul, Korea.
  Talk: "On surfaces of constant astigmatism"

- Mathematics in Armenia: Advances and Perspectives, August 2013, Tsaghkadzor, Armenia.
  Talk: "On surfaces of constant astigmatism"

- Mathematical Congress of the Americas (MCA), August 2013, Guanajuato, Mexico.
  Talk: "On surfaces of constant astigmatism"

- Geometry and Algebra of PDEs, August 2012, Tromsø, Norway.
  Talk: "Some results concerning the constant astigmatism equation"

- Algebra, Geometry and Mathematical Physics (AGMP), October 2011, Mulhouse, France.
  Talk: "A reciprocal transformation for the constant astigmatism equation"

10 Publications constituting the body of the thesis

Publications constituting the body of the thesis and my percentage contribution towards each of them are listed below.

- A. Hlaváč, More exact solutions of the constant astigmatism equation, *J. Geom. Phys.* **123** (2018), p. 209–220 .... **100** %
- A. Hlaváč and M. Marvan, Nonlocal conservation laws of the constant astigmatism equation, *J. Geom. Phys.* **113** (2017), p. 117–130 .. **50** %
- A. Hlaváč, On multisoliton solutions of the constant astigmatism equation, *J. Phys. A: Math. Theor.* **48** (2015) 365202 .... **100** %
- A. Hlaváč and M. Marvan, A reciprocal transformation for the constant astigmatism equation, *SIGMA* **10** (2014), 091 .... **75** %
- A. Hlaváč and M. Marvan, On Lipschitz solutions of the constant astigmatism equation, *J. Geom. Phys.* **85** (2014), p. 88–98 .... **25** %
- A. Hlaváč and M. Marvan, Another integrable case in two-dimensional plasticity, *J. Phys. A: Math. Theor.* **46** (2013) 045203 .... **50** %

11 Papers citing the publications constituting the body of the thesis

All citations without self-citations are listed below. By self-citations we mean references by a coauthor of the cited article.

- A. Hlaváč and M. Marvan, Another integrable case in two-dimensional plasticity, *J. Phys. A: Math. Theor.* **46** (2013) 045203

  is cited by:

1. N. Manganaro and M. Pavlov, The constant astigmatism equation. New exact solution, *J. Phys. A: Math. Theor.* **47** (2014) 075203.
2. M.V. Pavlov and S.A. Zykov, Lagrangian and Hamiltonian structures for the constant astigmatism equation, *J. Phys. A: Math. Theor.* **46** (2013) 395203.
3. S.I. Senashov and A. Yakhno, Some symmetry group aspects of a perfect plane plasticity system, *J. Phys. A: Math. Theor.* **46** (2013) 355202.

- A. Hlaváč and M. Marvan, A reciprocal transformation for the constant astigmatism equation, *SIGMA* **10** (2014), 091

  is cited by:

  1. N. Manganaro and M. Pavlov, The constant astigmatism equation. New exact solution, *J. Phys. A: Math. Theor.* **47** (2014) 075203.
  2. M.V. Pavlov and S.A. Zykov, Lagrangian and Hamiltonian structures for the constant astigmatism equation, *J. Phys. A: Math. Theor.* **46** (2013) 395203.

Regrettably, two more citations from authors Shou-Fu Tian, Li Zou and Tian-Tian Zhang of the paper "Lie symmetry analysis, conservation laws and analytical solutions for the constant astigmatism equation," Chin. J. Phys. 55 (2017) 1938–1952 are to be mentioned. Both of them refer to our two preprints

- A. Hlaváč and M. Marvan, Some results concerning the constant astigmatism equation, arXiv:1206.0321 (the content later published in [22] and [23]),
- A. Hlaváč and M. Marvan, A reciprocal transformation for the constant astigmatism equation, arXiv:1111.2027 (later published as [24]),

although the results from the preprints were already published in journals at that time. What is more, the results are ignored by the authors, as all CAE solutions from their paper had been published three years earlier in our work [23].

12 References

[1] M.J. Ablowitz, D.J. Kaup, A.C. Newell and H. Segur, Method for Solving the Sine-Gordon Equation, *Phys. Rev. Lett.* **30** (1973) 1262–1264.

[2] T. Aktosun, F. Demontis and C. van der Mee, Exact solutions to the sine-Gordon equation, *J. Math. Phys.* **51** (2010) 123521.

[3] R.L. Anderson and N.H. Ibragimov, *Lie-Bäcklund Transformations in Applications* (SIAM, 1979).

[4] A.V. Bäcklund, Om ytor med konstant negativ krökning, *Lunds Univ. Årsskrift,* **19** (1883) 1–48.

[5] H. Baran and M. Marvan, On integrability of Weingarten surfaces: a forgotten class, *J. Phys. A: Math. Theor.* **42** (2009) 404007.

[6] L. Bianchi, Ricerche sulle superficie elicoidali e sulle superficie a curvatura costante, *Ann. Scuola Norm. Sup. Pisa, I* **2** (1879) 285–341.

[7] L. Bianchi, Sulla trasformazione di Bäcklund per le superficie pseudosferiche, *Rend. Accad. Lincei* **5** (1892) 3–12.

[8] L. Bianchi, *Lezioni di Geometria Differenziale*, Vol. I (E. Spoerri, Pisa, 1903).

[9] L. Bianchi, *Lezioni di Geometria Differenziale*, Vol. II (E. Spoerri, Pisa, 1902).

[10] L. Bianchi, *Lezioni di Geometria Differenziale*, (E. Spoerri, Pisa, 1894). [German translation: *Vorlesungen über Differentialgeometrie*, (B.G. Teubner, Leipzig, 1899)]

[11] A.V. Bocharov, V.N. Chetverikov, S.V. Duzhin, N.G. Khor'kova, I.S. Krasil'shchik, A.V. Samokhin, Yu.N. Torkhov, A.M. Verbovetsky and A.M. Vinogradov, *Symmetries and Conservation Laws for Differential Equations of Mathematical Physics,* Transl. Math. Monographs 182 (Amer. Math. Soc., Providence, 1999).

[12] A.C. Bryan, On representations of the multisoliton solutions of the sine-Gordon equation, *Nonlinear Analysis, Theory, Methods & Applications*, Vol. **12**, No. 10. pp. 1047–1052, 1988

[13] P.J. Caudrey, J.D. Gibbon, J.C. Eilbeck, R.K.Bullough, Exact multi-soliton solutions of the self induced transparency and sine-Gordon equations, *Phys. Rev. Lett.* **30** (1973), 237–239.

[14] P.J. Caudrey, J.C. Eilbeck, J.D. Gibbon, R.K.Bullough, Multiple soliton and bisoliton bound state solutions of the sine-Gordon equation and related equations in nonlinear optics, *J. Phys. A: Math., Nucl. Gen.* **6** (1973), 112–114.

[15] P.J. Caudrey, J.C. Eilbeck, J.D. Gibbon, The sine-Gordon equation as a model classical field theory, *Nuovo Cimento,* **25** (1975), 497–512.

[16] A. S. Davydov, Solitons in molecular systems [in Russian], Naukova Dumka, Kiev (1984)

[17] B. Dubrovin and S. Natanzon, Real two-zone solutions of the sine-Gordon equation, *Funct. Anal. Appl.* **16** (1982) 21–33; transl. from *Funkts. Anal. Prilozh.* **16** (1982) 27–43.

[18] G. Ganchev and V. Mihova, On the invariant theory of Weingarten surfaces in Euclidean space, *J. Phys. A: Math. Theor.* **43** (2010) 405210.

[19] Goursat E., Le Problème de Bäcklund, Gauthier-Villars, Paris, 1925.

[20] I. V. Gribkov, Some solutions of the sine-Gordon equation obtained by means of a Bäcklund transformation, *Uspekhi Mat. Nauk*, **33**:2(200) (1978), 191–192; Russian Math. Surveys, **33**:2 (1978), 231–232.

[21] R. Hirota, Exact Solution of the Sine-Gordon Equation for Multiple Collisions of Solitons, *Journ. Phys. Soc. Japan* **33** (1972) 1459–1463.

[22] A. Hlaváč and M. Marvan, Another integrable case in two-dimensional plasticity, *J. Phys. A: Math. Theor.* **46** (2013) 045203.

[23] A. Hlaváč and M. Marvan, On Lipschitz solutions of the constant astigmatism equation, *Journal of Geometry and Physics* **85** (2014), p. 88–98.

[24] A. Hlaváč and M. Marvan, A reciprocal transformation for the constant astigmatism equation, *SIGMA* **10** (2014), 091.

[25] A. Hlaváč, On multisoliton solutions of the constant astigmatism equation, *J. Phys. A: Math. Theor.* **48** (2015) 365202.

[26] A. Hlaváč and M. Marvan, Nonlocal conservation laws of the constant astigmatism equation, *Journal of Geometry and Physics* **113** (2017), p. 117–130.

[27] A. Hlaváč, More exact solutions of the constant astigmatism equation, *Journal of Geometry and Physics* **123** (2018), p. 209–220.

[28] C.A. Hoenselaers and S. Miccichè, Transcendental solutions of the sine-Gordon equation, in: A. Coley, D. Levi, R. Milson, C. Rogers and P. Winternitz, eds., *Bäcklund and Darboux transformations. The geometry of solitons*, AARMS-CRM Workshop, Halifax, 1999, CRM Proc. Lecture Notes 29 (Amer. Math. Soc., Providence, RI, 2001) 261–271.

[29] J.G. Kingston and C. Rogers, Reciprocal Bäcklund transformations of conservation laws, *Phys. Lett. A* **92** (1982) 261–264.

[30] I.S. Krasil'shchik and A.M. Vinogradov, Nonlocal trends in the geometry of differential equations: Symmetries, conservation laws, and Bäcklund transformations, *Acta Appl. Math.* **15** (1989) 161–209.

[31] T. Kuen, Ueber Flächen von constantem Krümmungsmaass, *Jahrbuch über die Fortschritte der Mathematik* **16** (1884) 193–206.

[32] R. von Lilienthal, Bemerkung über diejenigen Flächen bei denen die Differenz der Hauptkrümmungsradien constant ist, *Acta Mathematica* **11** (1887) 391–394.

[33] R. Lipschitz, Zur Theorie der krummen Oberflächen, *Acta Math.* **10** (1887) 131–136.

[34] N. Manganaro and M. Pavlov, The constant astigmatism equation. New exact solution, *J. Phys. A: Math. Theor.* **47** (2014) 075203.

[35] A. Mannheim, Sur les surfaces dont les rayons de courbure principaux sont fonctions l'un de l'autre, *Bull. S. M. F.* **5** (1877) 163–166.

[36] M. Marvan, A direct procedure to compute zero-curvature representations. The case sl_2, in: *Secondary Calculus and Cohomological Physics,* Proc. Conf. Moscow, 1997 (ELibEMS, 1998) pp. 10, `www.emis.de/proceedings/SCCP97`.

[37] M. Marvan, Some local properties of Bäcklund transformations, *Acta Appl. Math.* **54** (1998) 1–25.

[38] F. Minding, Wie sich entscheiden lässt, ob zwei gegebene krumme Flächen auf einander abwickelbar sind oder nicht; nebst Bemerkungen über die Flächen von unveränderlichem Krümmungsmaaße, *Journal für die reine und angewandte Mathematik* **19** (1839) 370–383.

[39] A.P. Norden, The Theory of Surfaces [in Russian], (GITTL, Moscow, 1956).

[40] A. Ovchinnikov, Gallery of pseudospherical surfaces, in: D. Wójcik and J. Cieśliński, *Nonlinearity & Geometry, Luigi Bianchi Days*, Proc. 1st Non-Orthodox School, Warsaw, September 21–28, 1995 (Polish Scientific, Warsaw, 1998) 41–60.

[41] M.V. Pavlov and S.A. Zykov, Lagrangian and Hamiltonian structures for the constant astigmatism equation, *J. Phys. A: Math. Theor.* **46** (2013) 395203.

[42] A.G. Popov and E.V. Maevskii, Analytical approaches to the study of the sine-Gordon equation and pseudospherical surfaces, *J. Math. Sci.* **142** (2007) 2377–2418.

[43] R.O. Popovych, N.M. Ivanova, Hierarchy of conservation laws of diffusion-convection equations, *J. Math. Phys.* **46** (2005) 043502.

[44] A. Ribaucour, Note sur les développées des surfaces, *C. R. Acad. Sci. Paris* **74** (1872) 1399–1403.

[45] C. Rogers and W.K. Schief, *Bäcklund and Darboux Transformations. Geometry and Modern Applications in Soliton Theory* (Cambridge Univ. Press, Cambridge, 2002).

[46] G. Roth-Kleyer, ed., *Göttinger Sammlung matematischer Modelle* (Göttingen collection of mathematical models), `http://www.uni-math.gwdg.de/modellsammlung/`.

[47] M.A. Sadowsky, Equiareal pattern of stress trajectories in plane plastic strain, *J. Appl. Mech.* **8** (1941) A-74–A-76.

[48] M.A. Sadowsky, Equiareal patterns, *Amer. Math. Monthly* **50** (1943) 35–40.

[49] M.I. Serov and L.M. Blazhko, Nonlocal formulas for the propagation of solutions and the conditional symmetry of the sine-Gordon equation. (Ukrainian) *Ukr. Mat. Visn.* **6** (2009), no. 4, 531–552, 582; translation in *Ukr. Math. Bull.* **6** (2009), no. 4, 527548.

[50] A. Sym, Soliton surfaces and their applications. Soliton geometry from spectral problems, in: R. Martini, ed., *Geometric Aspects of the Einstein Equations and Integrable Systems,* Lecture Notes in Physics 239 (Springer, Berlin, 1985) 154–231.

[51] C.E. Weatherburn, *Differential Geometry of Three Dimensions* (Cambridge University Press, Cambridge, 1927).

[52] Z.H. Xie, P.R. Munroe, D. Mcgrouther, R.K. Singh, M. Hoffman, A. Bendavid, P.J. Martin and S. Yew, Three-dimensional study of indentation-induced cracks in an amorphous carbon coating on a steel substrate, *J. Mater. Res.* **21** (2006) 2600–2605.

[53] A. Yonezu, Ling Liu and Xi Chen, Analysis on spiral crack in thick diamond-like carbon film subjected to spherical contact loading, *Mat. Sci. Eng. A* **496** (2008) 67–76.

[54] S.A. Zadadaev, Traveling Wave Type Solutions to the sin-Gordon Equation and Pseudospherical Surfaces, *Moscow University Mathematics Bulletin* **49** (1994) 34–40.

[55] V.E. Zakharov, A.B. Shabat, Integration of nonlinear equations of mathematical physics by the method of inverse scattering. II, *Funkts. Anal. Prilozh.* **13** (3) (1979) 1322 (in Russian); English translation *Funct. Anal. Appl.* **13** (1979) 166174.

[56] M. G. Zelin, Topographic study of superplastically formed AA7475 hemispherical domes, *J. Material Sci.* **31** (1996) 843–849.